CHAPTER 4 - EXPERIMENT 2

CHARACTERIZATION OF THE MICROSTRUCTURE AND MECHANICAL PROPERTIES OF LIQUID PHASE DIFFUSION BONDS USING EUTECTIC Ni-Hf AND Ni-Zr BRAZE ALLOYS AFTER SHORT PROCESSING TIMES (40 MINUTES)

This chapter examines the microstructure and mechanical properties of liquid phase diffusion bonds, produced by mixing the novel eutectic Ni-Hf or Ni-Zr braze alloys with MarM247 Ni-base superalloy powder, after short processing times (40 minutes) at 1230°C.

4.1) Introduction

As shown in the preceding chapter, simple binary eutectic Ni-Hf and Ni-Zr braze alloys can be used to successfully join In738 Ni-base superalloy. The joint gap must, however, be narrow (less than 0.15 mm in width) to allow capillary action to draw the filler metal into the joint. Such narrow joint gaps are usually only found in the manufacturing industry. In the repair industry, especially in IGT (industrial gas turbine) engine components, cracks are frequently wider than 0.15 mm and the simple eutectic Ni-Hf and Ni-Zr brazes will most likely not deliver adequate mechanical properties if used independently. In order to improve the mechanical properties of the In738 braze joints, the Ni-Hf or Ni-Zr eutectic braze alloy was mixed with MarM247 Ni-base superalloy powder, and processed using the liquid phase diffusion bonding (LPDB) process described in §1.6 of the literature survey.

The objectives of Experiment 2 were therefore:

- to demonstrate that the novel Ni-Hf and Ni-Zr braze alloys can be used in conjunction with MarM247 Ni-base superalloy powder to successfully join In738 using the liquid phase diffusion bonding (LPDB) process, and
- to examine the microstructure and mechanical properties of the LPDB joints after short processing times (40 minutes).

4.2) Experimental procedure

In738 plate material was produced and prepared as described in §3.2. A mixture of coarse (+325 mesh) and fine (–325 mesh) MarM247 Ni-base superalloy powder with a nominal composition shown in Table 10 was mixed with braze binder to form a paste. MarM247 powder, as opposed to In738, was selected because MarM247 is recognized as the equiaxed Ni-base superalloy with the highest mechanical integrity. The MarM247 paste was applied to the In738 plate over an area of approximately 2500 mm^2 and allowed to dry. A layer of eutectic Ni-Hf or Ni-Zr braze alloy in paste form (produced as described in §3.2) was then applied over the dry MarM247 powder. The samples were dried for one hour, and placed into a laboratory vacuum furnace.

Table 10 – Nominal chemical composition of the MarM247 powder used in this investigation (wt.%, balance Ni).

B	C	Co	Cr	Hf	Mo	Al	W	Ta	Ti	Zr	Fe
0.001	0.15	10.0	8.25	1.50	0.70	5.50	10.0	3.0	1.0	0.05	0.5

The vacuum braze cycle used for both braze alloys was as follows:

1) Ramp up to a temperature of 450°C at a minimum rate of 9°C/minute.
2) Hold at 450°C for 20 minutes to allow the binder to burn off.
3) Ramp up to a temperature of 1150°C at a minimum rate of 9°C/minute.
4) Hold at 1150°C for 20 minutes to allow the samples to stabilize at this temperature.
5) Ramp up to a temperature of 1230°C at a minimum rate of 9°C/minute to melt the Ni-Hf and Ni-Zr braze alloys and to allow the melt to infiltrate the MarM247 powder.
6) Hold at 1230°C for 40 minutes.
7) Furnace cool to room temperature.

After exposing the In738 plates to the vacuum LPDB cycle described above, samples were sectioned and mounted using conventional metallographic practices. The mounted samples were polished and etched with Marble's reagent to reveal the microstructure. Optical and scanning electron microscopy techniques were then used to characterize the microstructures.

Tensile tests were performed at room temperature (21°C) and at temperatures of 540°C, 650°C, 760°C, 870°C and 980°C. In order to produce the tensile specimens, MarM247 plate material was joined using the procedure described earlier. The tensile test samples were aged at 870°C for 20 hours, as is typical during a normal braze repair cycle. The tensile test specimens were prepared in a butt joint configuration, shown schematically in **Figure 69**. The LPDB joint was 1.5 mm wide to simulate the typical crack widths found in Industrial Gas Turbine (IGT) components, and was located in the centre of the sample gauge length.

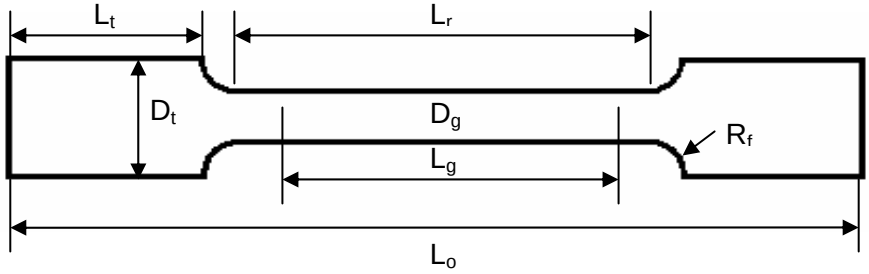

Figure 69 – Configuration of tensile and creep rupture specimens: D_g = 4.6 mm; L_g = 18.3 mm; L_r = 21.8 mm; L_o = 46.5 mm; R_f = 3.2 mm; L_t = 9.5 mm; and D_t = 8 mm.

4.3) Results and discussion

4.3.1 Microstructural investigation:

The microstructure of the LPDB joint produced with Ni-Hf braze filler metal and MarM247 powder is shown in **Figures 70 to 75**. The equiaxed, light-etching particles are the original MarM247 powder particles, and the darker areas consist of eutectic Ni-Hf braze alloy. The variation in MarM247 particle size, evident in **Figures 71 and 72**, is due to the mixture of coarse and fine MarM247 powders used in producing the superalloy powder. Such a mixture results in a denser, less porous structure, provided the braze temperature is high enough and the Ni-Hf braze alloy has sufficient time to flow.

Figures 72 and 73 indicate that the Ni-Hf joint is composed of MarM247 powder particles, interspersed with a thick layer consisting of γ dendrites and an intermetallic Ni_5Hf or Ni_7Hf_2

phase. It is expected that the mechanical properties of this joint will fall between those of the MarM247 superalloy and the Ni-Hf braze alloy. The dark etching component in **Figures 74 and 75** most likely consists of proeutectic γ, and the γ-Ni_5Hf or γ-Ni_7Hf_2 eutectic component. The γ dendrites and the Ni_5Hf or Ni_7Hf_2 phase surround each MarM247 powder particle, resembling a film or coating around the particles. If this film is brittle, cracks can propagate around each powder particle and connect to form what is referred to in industry as craze-cracked areas.

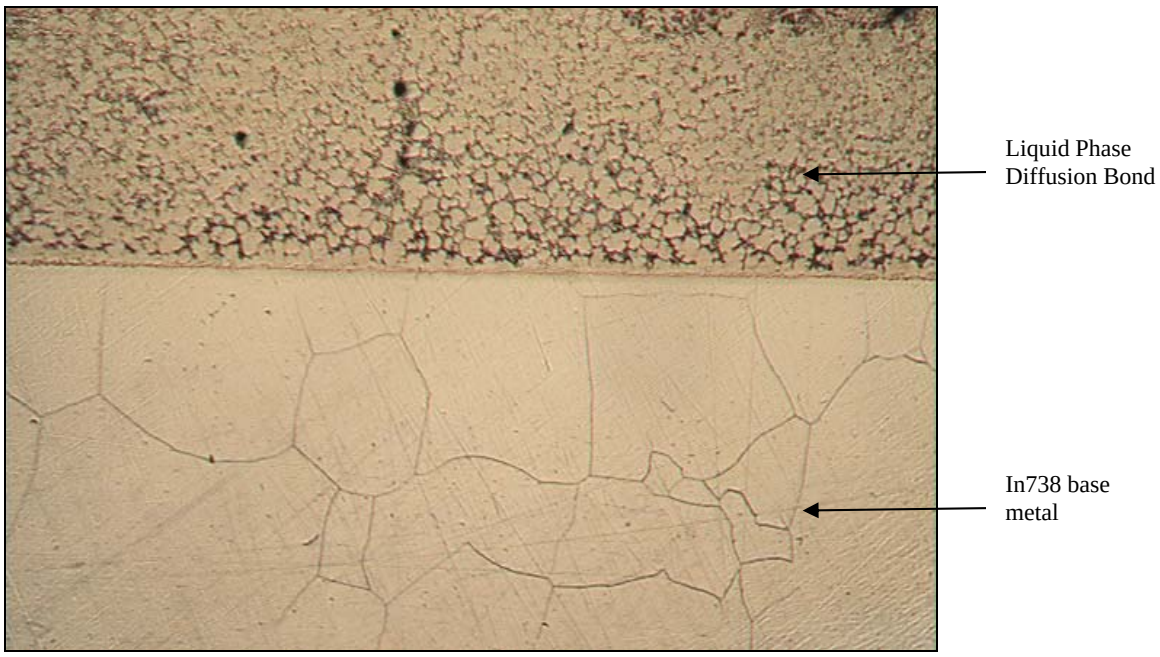

Figure 70 – Ni-Hf braze dispersed between MarM247 powder particles after brazing at 1230°C for 40 minutes. Magnification: 50X.

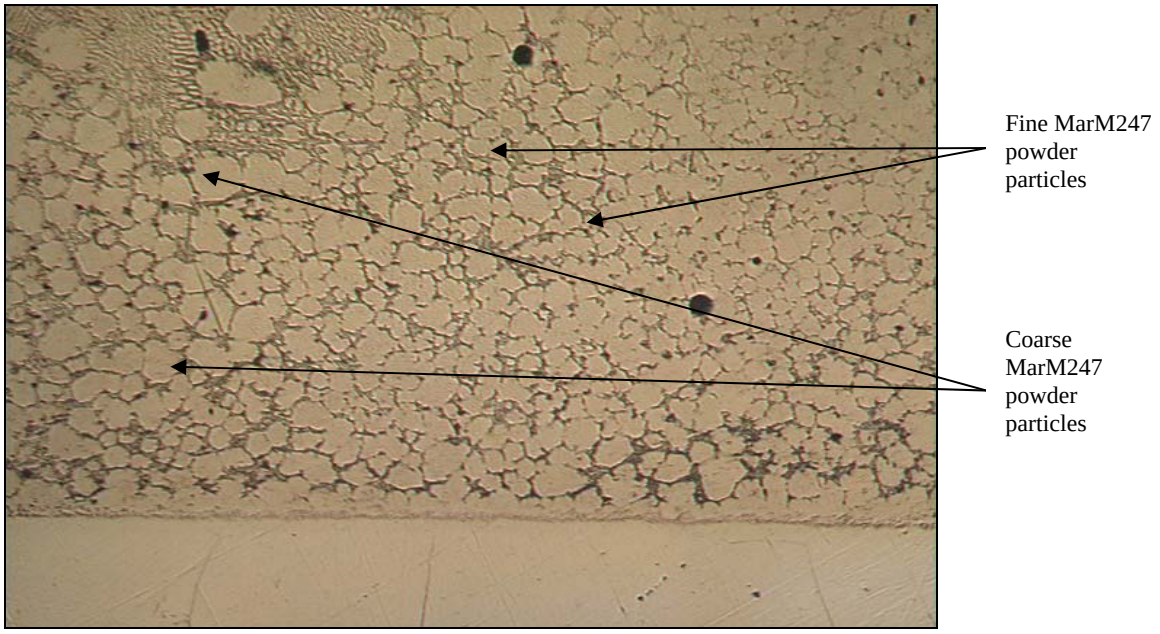

Figure 71 - Ni-Hf braze dispersed between MarM247 powder particles after brazing at 1230°C for 40 minutes. Magnification: 100X.

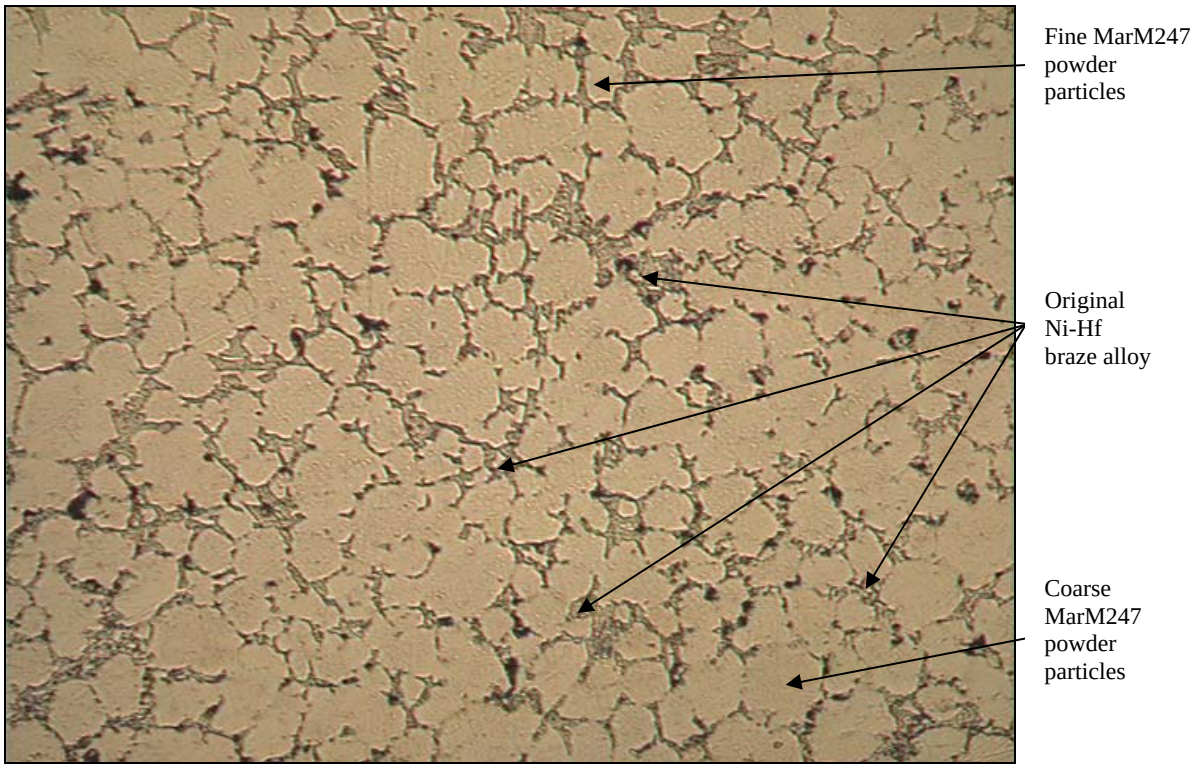

Figure 72 - Ni-Hf braze dispersed between MarM247 powder particles after brazing at 1230°C for 40 minutes. Magnification: 200X.

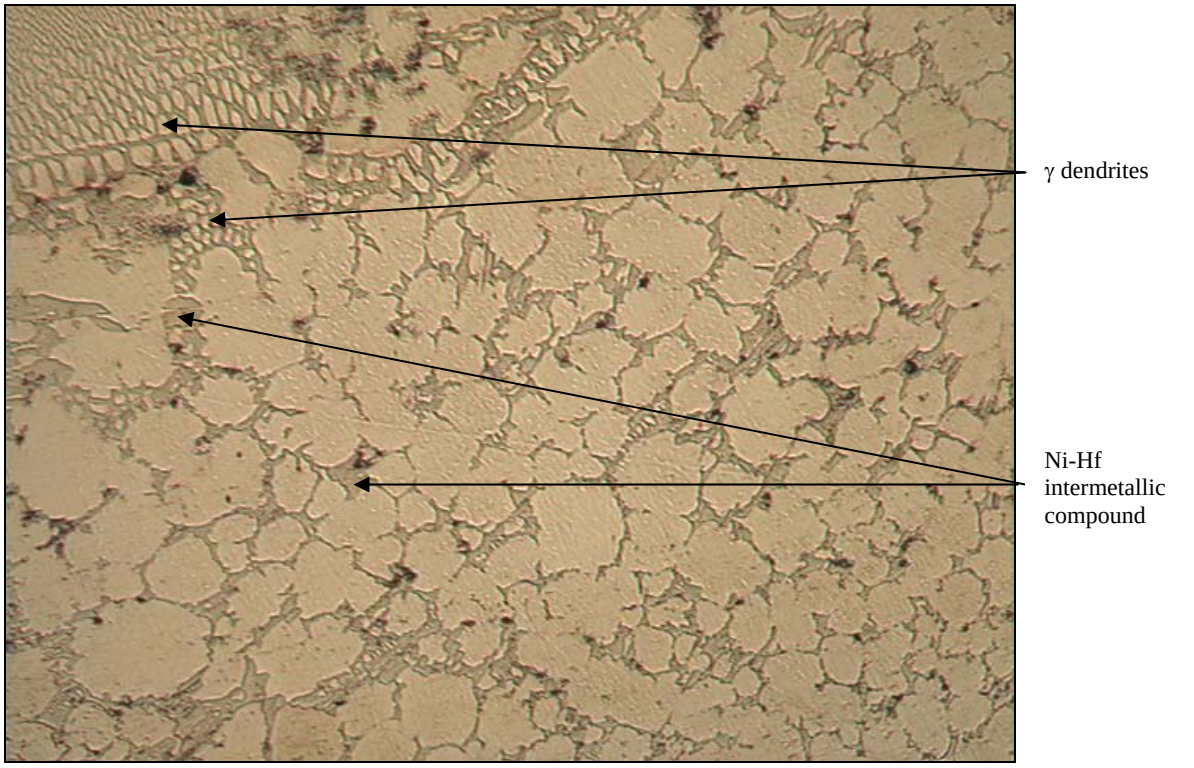

Figure 73 - Ni-Hf braze dispersed between MarM247 powder particles after brazing at 1230°C for 40 minutes. Magnification: 200X.

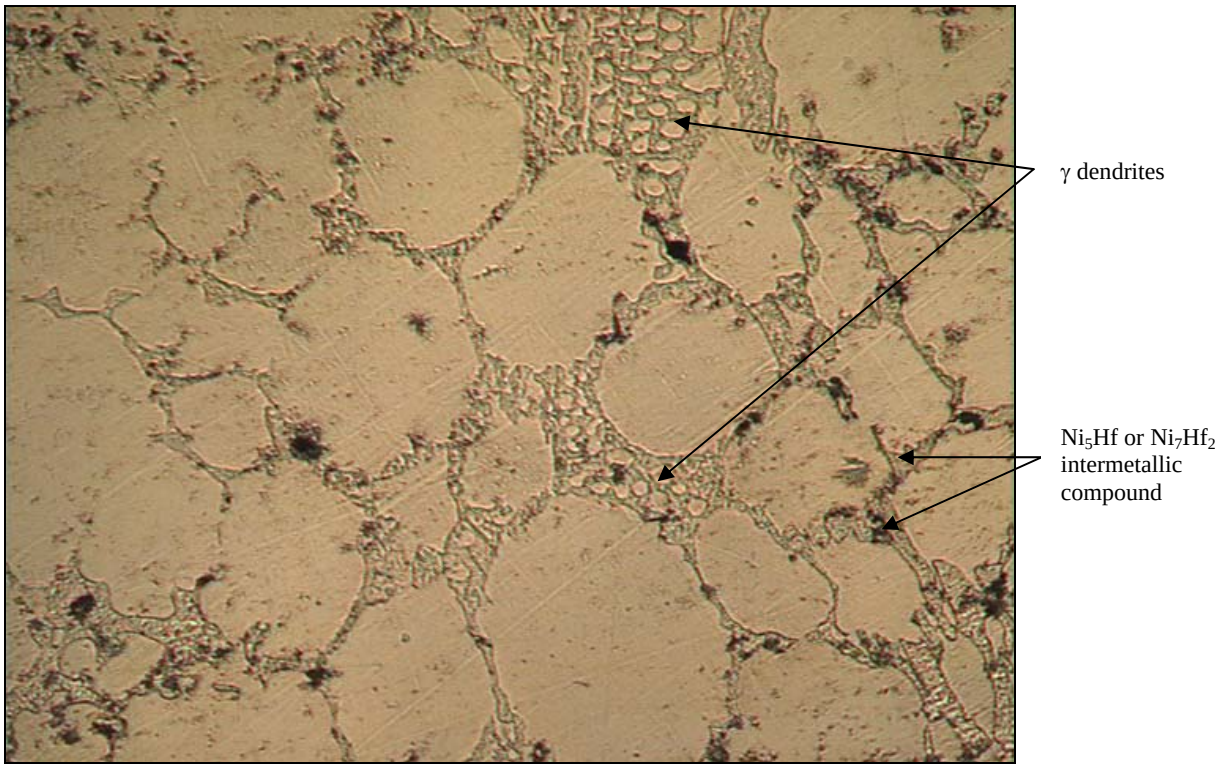

Figure 74 - Ni-Hf braze dispersed between MarM247 powder particles after brazing at 1230°C for 40 minutes. Magnification: 500X.

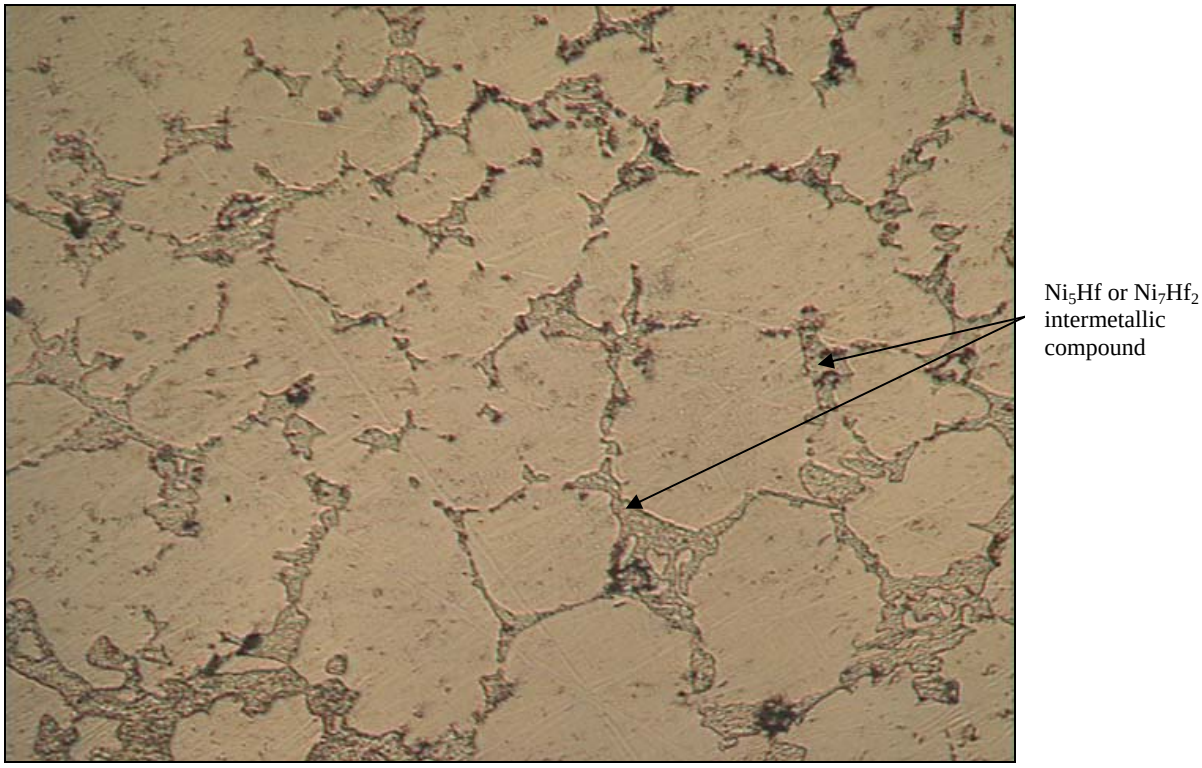

Figure 75 - Ni-Hf braze dispersed between MarM247 powder particles after brazing at 1230°C for 40 minutes. Magnification: 500X.

The microstructure of the LPDB joint produced using MarM247 powder and Ni-Zr braze paste is shown in **Figures 76 to 81** at various magnifications. The original MarM247 powder particles are evident as the lighter, more equiaxed component, while the darker regions consist of eutectic Ni-Zr braze alloy. As explained earlier, the variation in MarM247 particle size is due to the mixture of coarse and fine powders in the joint. This ensure a denser, less porous structure, provided the braze temperature is high enough and the Ni-Zr braze alloy has sufficient time to flow during the braze cycle.

Figures 78 to 81 illustrate that the joint is composed of individual MarM247 powder particles, separated by a layer consisting of γ dendrites and Ni_5Zr intermetallic compound (darker regions). Since this layer surrounds each MarM247 particle, its properties will most likely influence the properties of the joint. A brittle film will promote the propagation of cracks and may lead to the development of craze-cracked areas in service.

Figure 82 displays a SEM micrograph of the MarM247/Ni-Hf joint after brazing at 1230^{o}C for 40 minutes. SEM-EDS analysis was performed on two phases, highlighted by the arrows in **Figure 82**. One phase was arbitrarily labelled "grain boundary particle", and was shown to consist of 78.06Ni-6.68Co-3.74Cr-4.22Al-2.42W-3.01Fe-0.79Mo-0.81Ti-0.27Zr (wt.%). On the basis of this composition, the "grain boundary particle" phase was identified as γ. The second phase was arbitrarily labelled "grain boundary film", and contained 50.31Ni-43.93Hf-2.32W-2.50Co-0.40Cr-0.39Al-0.14Ti (wt.%). According to the Ni-Hf phase diagram (shown in **Figure 49**), the Ni_7Hf_2 intermetallic phase contains approximately 46.5% Hf, whereas the Ni_5Hf phase contains about 37.9% Hf. On the basis of the SEM-EDS analysis, the "grain boundary film" phase was therefore provisionally identified as the Ni_7Hf_2 intermetallic phase, with some W, Co, Cr, Al and Ti in solution.

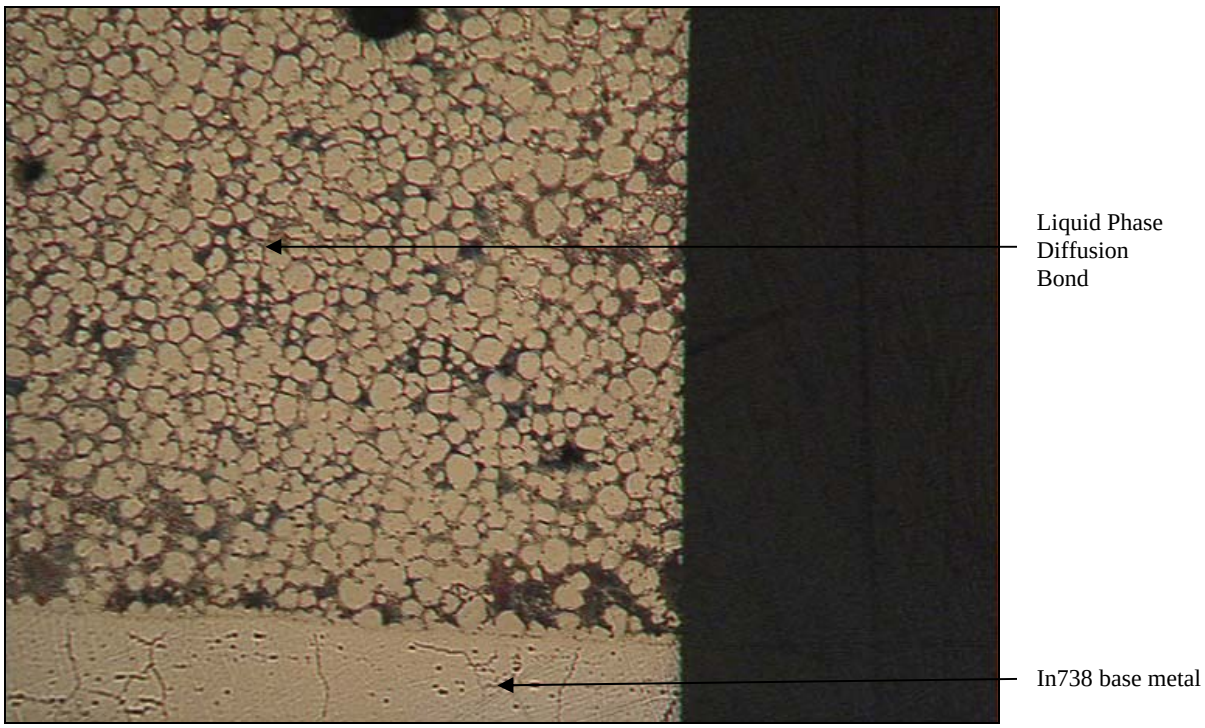

Figure 76 - Ni-Zr braze dispersed between MarM247 powder particles after brazing at 1230°C for 40 minutes. Magnification: 50X.

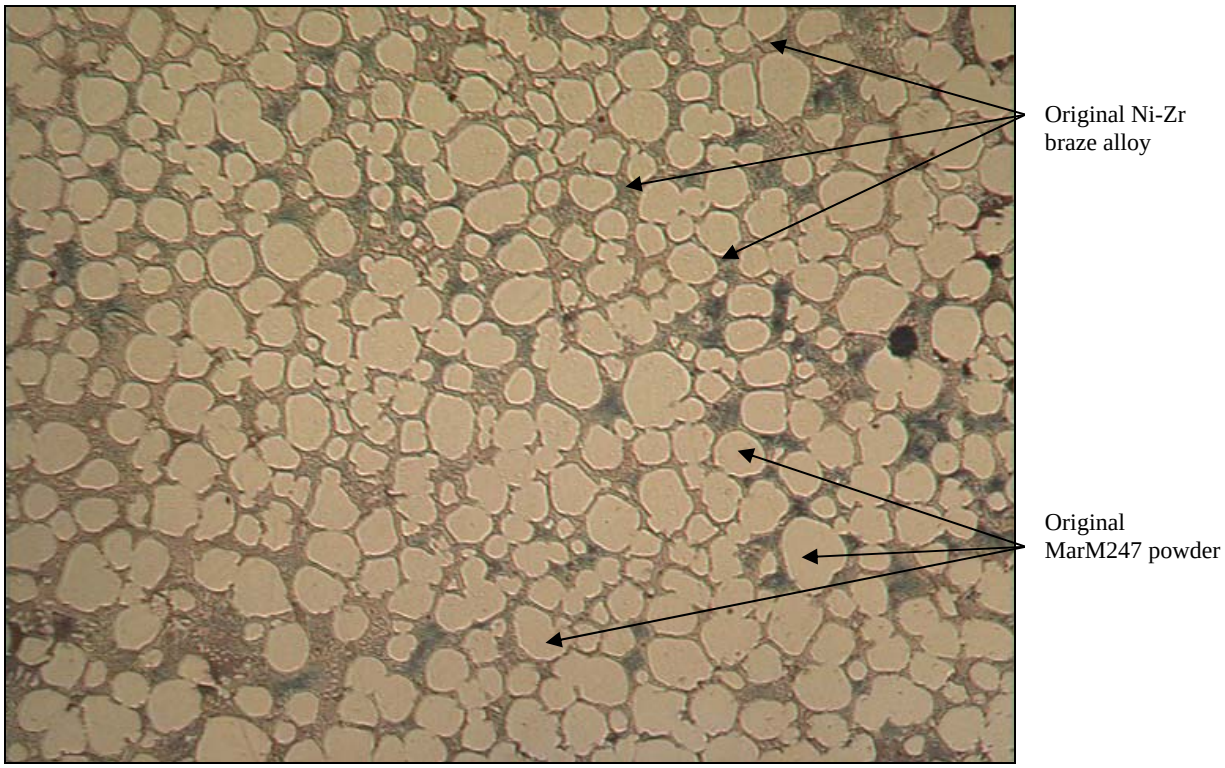

Figure 77 - Ni-Zr braze dispersed between MarM247 powder particles after brazing at 1230°C for 40 minutes. Magnification: 100X.

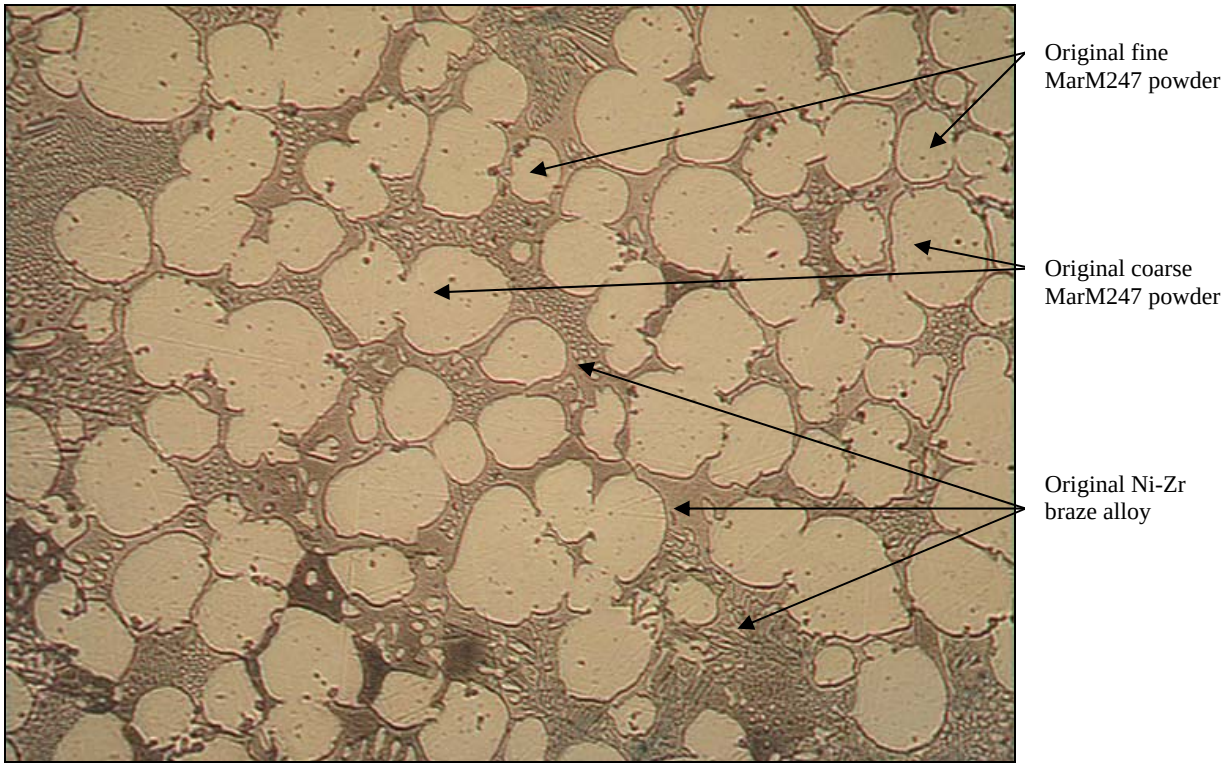

Figure 78 - Ni-Zr braze dispersed between MarM247 powder particles after brazing at 1230°C for 40 minutes. Magnification: 200X.

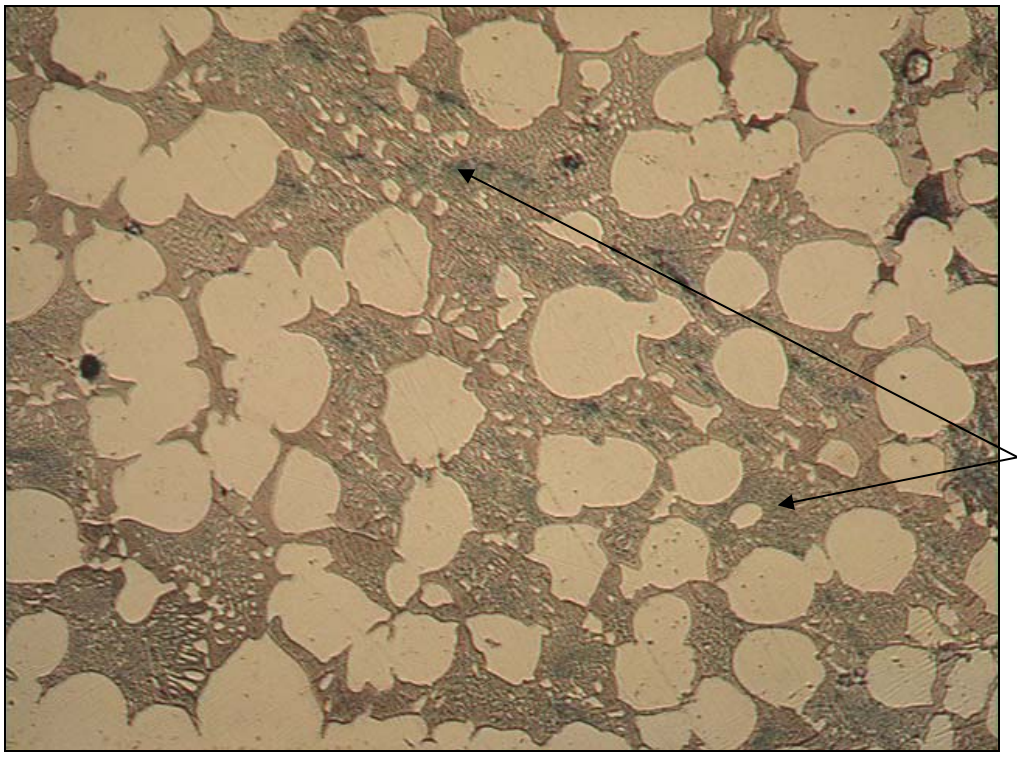

Figure 79 - Ni-Zr braze dispersed between MarM247 powder particles after brazing at 1230°C for 40 minutes. Magnification: 200X.

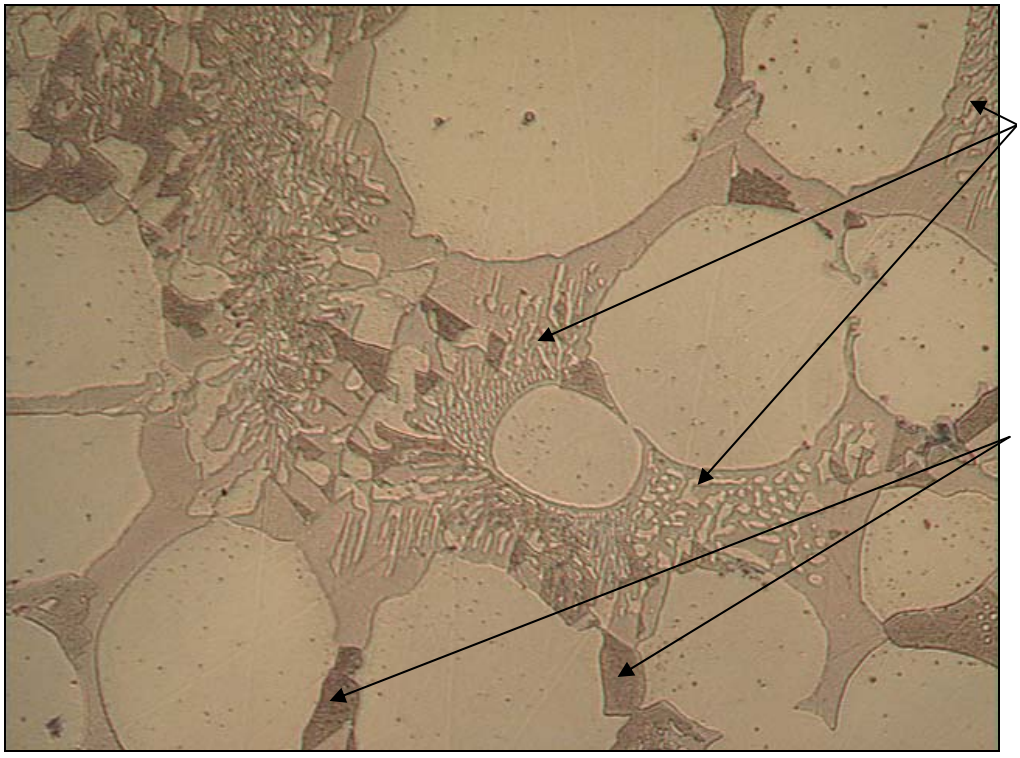

Figure 80 - Ni-Zr braze dispersed between MarM247 powder particles after brazing at 1230°C for 40 minutes. Magnification: 500X.

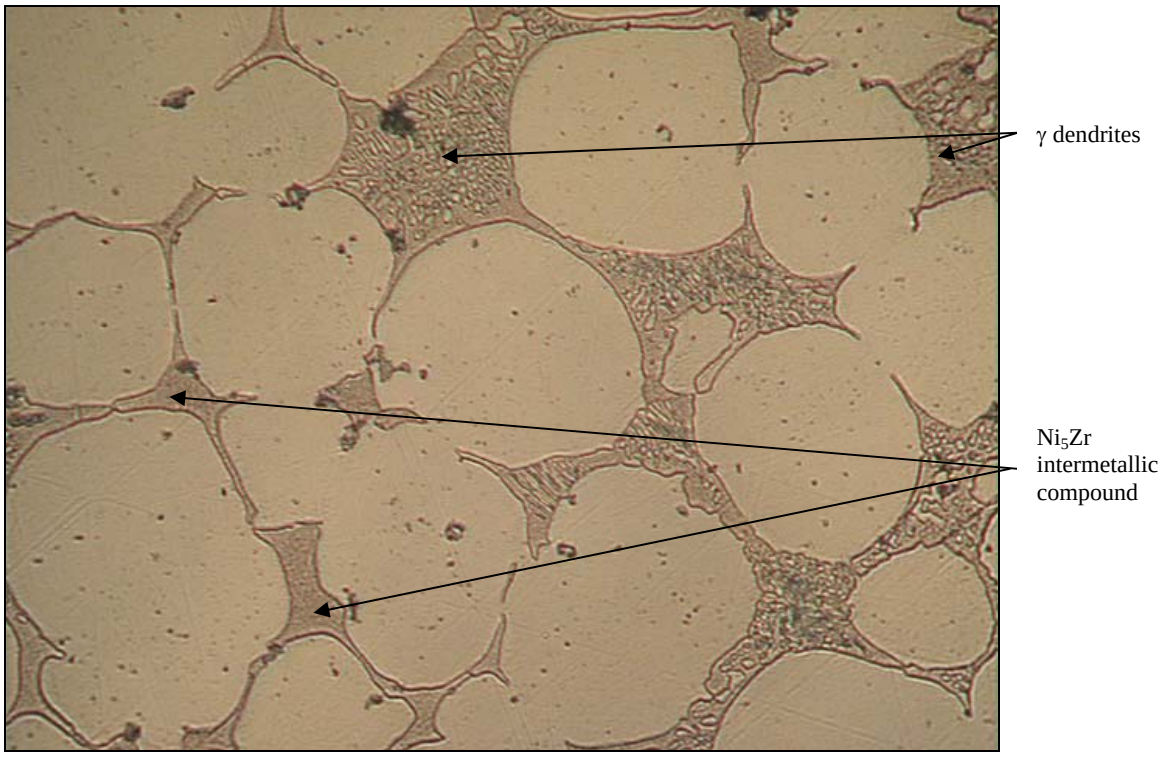

Figure 81 - Ni-Zr braze dispersed between MarM247 powder particles after brazing at 1230°C for 40 minutes. Magnification: 500X.

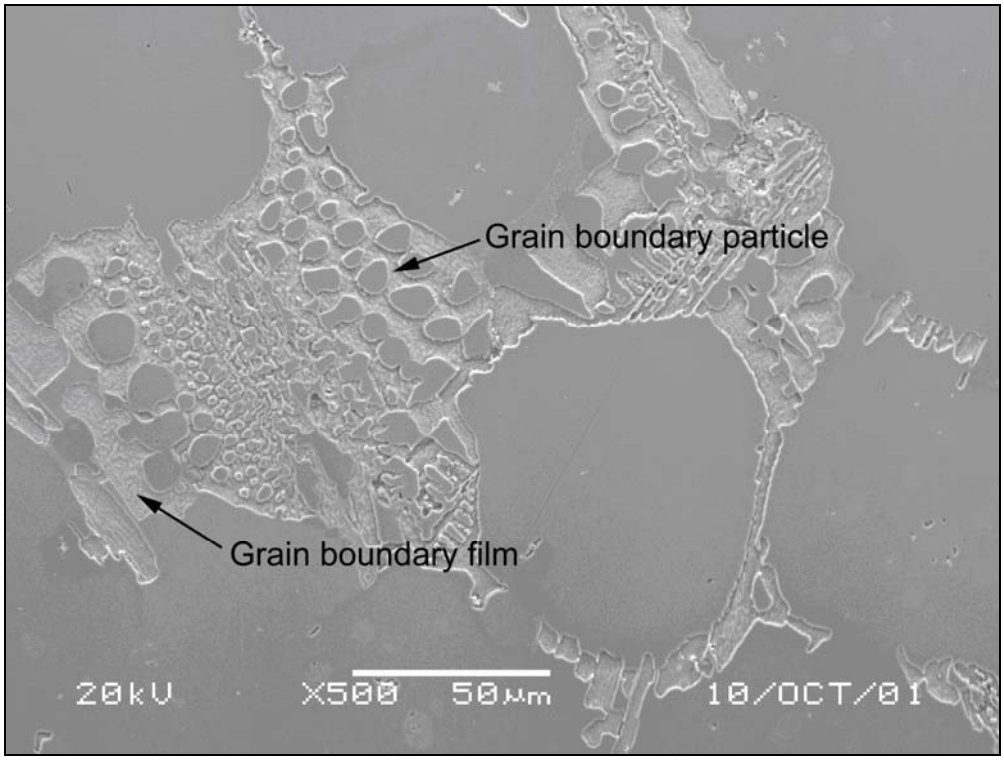

Figure 82 – SEM micrograph of the Ni-Hf braze, showing the phases identified as γ (labelled "grain boundary particle") and Ni_7Hf_2 (labelled "grain boundary film").

Figure 83 displays a SEM micrograph of the MarM247/Ni-Zr joint brazed at 1230°C for 40 minutes. Two phases, highlighted by the arrows in **Figure 83,** were analyzed using the SEM-EDS technique. The phase arbitrarily labelled "grain boundary particle" was identified as γ dendrites (with a composition of 74.48Ni-8.76Zr-5.64Co-3.21Cr-3.27Al-2.26W-1.86Mo-0.52Ti). The second phase, arbitrarily labelled "grain boundary film", had a composition of 69.49Ni-24.24Zr-2.03W-2.99Co-0.62Cr-0.41Mo-0.21Ti (wt.%). This phase was identified as the Ni_5Zr intermetallic phase, with small amounts of W, Co, Cr and Mo in solution.

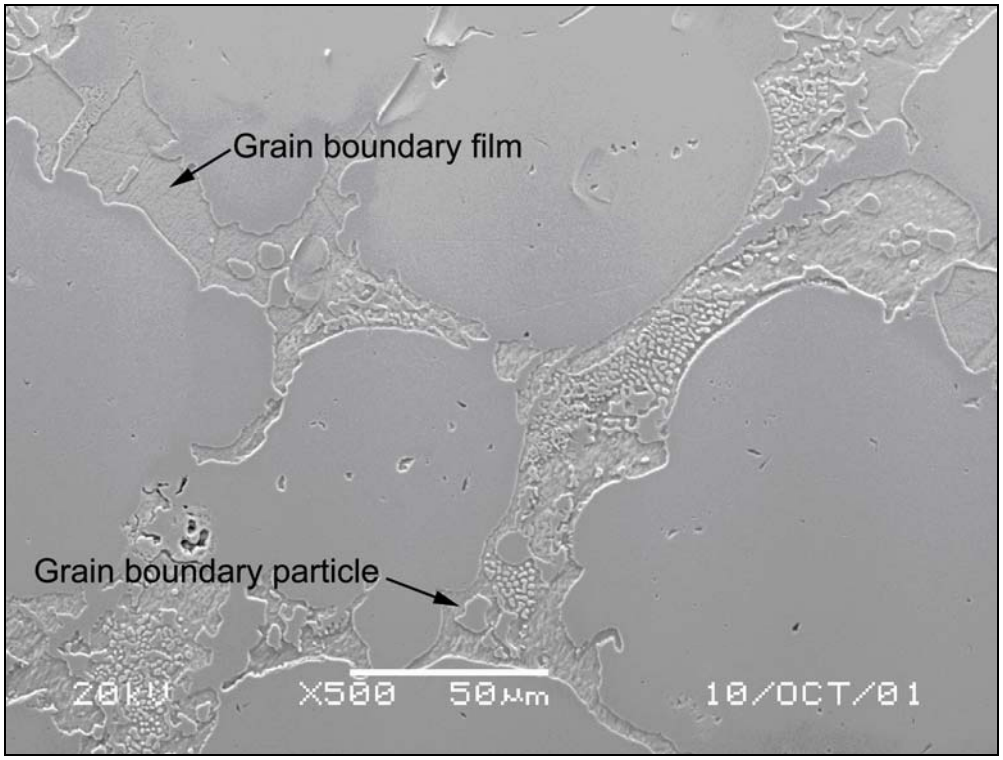

Figure 83 – SEM micrograph of the Ni-Zr braze, showing the phases identified as γ (labelled "grain boundary particle") and Ni_5Zr (labelled "grain boundary film").

4.3.2 Tensile test results:

The results of tensile tests performed at various temperatures are shown in **Tables 11 to 16**, and displayed graphically in **Figures 84 and 85**. The values shown represent the average of three tests.

Table 11 – Joint tensile properties measured at 21°C.

Tensile properties	Ni-Hf joints	Ni-Zr joints	MarM247 base metal
Tensile Strength (UTS)	323 MPa (46.8 ksi)	557 MPa (80.7 ksi)	960 MPa (139 ksi)
Yield Strength (YS)	239 MPa (34.7 ksi)	505 MPa (73.2 ksi)	800 MPa (116 ksi)
Elongation (%)	4.7	3.0	7.9
Reduction in area (RA) %	6.3	4.4	10.0

Table 12 – Joint tensile properties measured at 540°C.

Tensile properties	Ni-Hf joints	Ni-Zr joints	MarM247 base metal
Tensile Strength (UTS)	328 MPa (47.6 ksi)	619 MPa (89.7 ksi)	1014 MPa (147 ksi)
Yield Strength (YS)	243 MPa (35.2 ksi)	539 MPa (78.1 ksi)	801 MPa (116 ksi)
Elongation (%)	3.8	2.7	7.8
Reduction in area (RA) %	4.2	3.2	9.9

Table 13 – Joint tensile properties measured at 650°C.

Tensile properties	Ni-Hf joints	Ni-Zr joints	MarM247 base metal
Tensile Strength (UTS)	343 MPa (49.7 ksi)	562 MPa (81.4 ksi)	1040 MPa (151 ksi)
Yield Strength (YS)	265 MPa (38.4 ksi)	513 MPa (74.4 ksi)	805 MPa (117 ksi)
Elongation (%)	2.8	2.2	7.0
Reduction in area (RA) %	3.6	2.9	9.7

Table 14 – Joint tensile properties measured at 760°C.

Tensile properties	Ni-Hf joints	Ni-Zr joints	MarM247 base metal
Tensile Strength (UTS)	333 MPa (48.3 ksi)	593 MPa (85.9 ksi)	1000 MPa (145 ksi)
Yield Strength (YS)	282 MPa (40.8 ksi)	553 MPa (80.1 ksi)	815 MPa (118 ksi)
Elongation (%)	2.5	1.2	6.0
Reduction in area (RA) %	3.2	5.9	8.4

Table 15 – Joint tensile properties measured at 870°C.

Tensile properties	Ni-Hf joints	Ni-Zr joints	MarM247 base metal
Tensile Strength (UTS)	289 MPa (41.9 ksi)	444 MPa (64.4 ksi)	790 MPa (115 ksi)
Yield Strength (YS)	211 MPa (30.5 ksi)	414 MPa (60.0 ksi)	650 MPa (94 ksi)
Elongation (%)	2.0	1.0	5.0
Reduction in area (RA) %	3.0	2.4	7.7

Table 16 – Joint tensile properties measured at 980°C.

Tensile properties	Ni-Hf joints	Ni-Zr joints	MarM247 base metal
Tensile Strength (UTS)	195 MPa (28.3 ksi)	261 MPa (37.8 ksi)	506 MPa (73 ksi)
Yield Strength (YS)	141 MPa (20.4 ksi)	245 MPa (35.5 ksi)	312 MPa (45 ksi)
Elongation (%)	1.8	0.8	4.7
Reduction in area (RA) %	2.9	1.9	7.5

As shown in **Table 11**, the room temperature tensile and yield strengths of the Ni-Hf LPDB joints were 34% and 30%, respectively, of those of the MarM247 base metal, whereas the tensile and yield strengths of the Ni-Zr joints were 58% and 63%, respectively, of those of the MarM247 base metal. The Ni-Hf joints therefore exhibited considerably lower strength than the Ni-Zr joints after short processing times (40 minutes). The Ni-Hf joints, however, exhibited approximately 60% of the ductility of the MarM247 base metal, whereas the Ni-Zr joints only displayed about 40% of the base metal's ductility. It should be noted that, after

short processing times, the ductility of the Ni-Zr and Ni-Hf joints was significantly higher than the ductility of similar joints containing boron as melt point depressant. Boron-containing joints typically exhibit ductility values in the range of 0.5 to 1.0% after short processing times [35-37]. This observation provides initial evidence that, if higher strength joints can be achieved by increasing the processing time and similar levels of ductility are obtained, the use of Zr or Hf as melt point depressant in Ni-base braze alloys (instead of B) holds considerable potential for crack repair in the IGT industry.

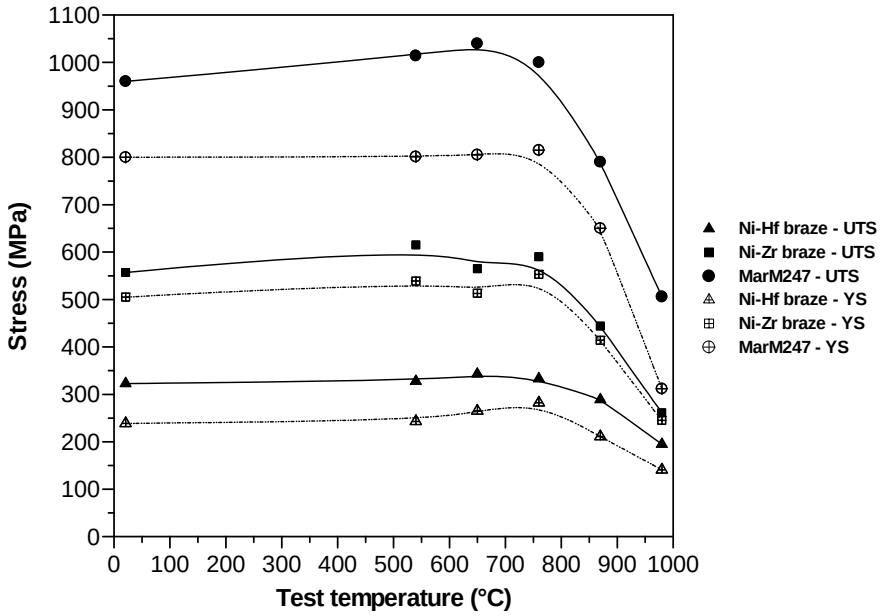

Figure 84 – The tensile strength (UTS) and yield strength (YS) of the Ni-Hf and Ni-Zr braze joints and the MarM247 parent metal as a function of the test temperature (each data point shown represents the average of three tests).

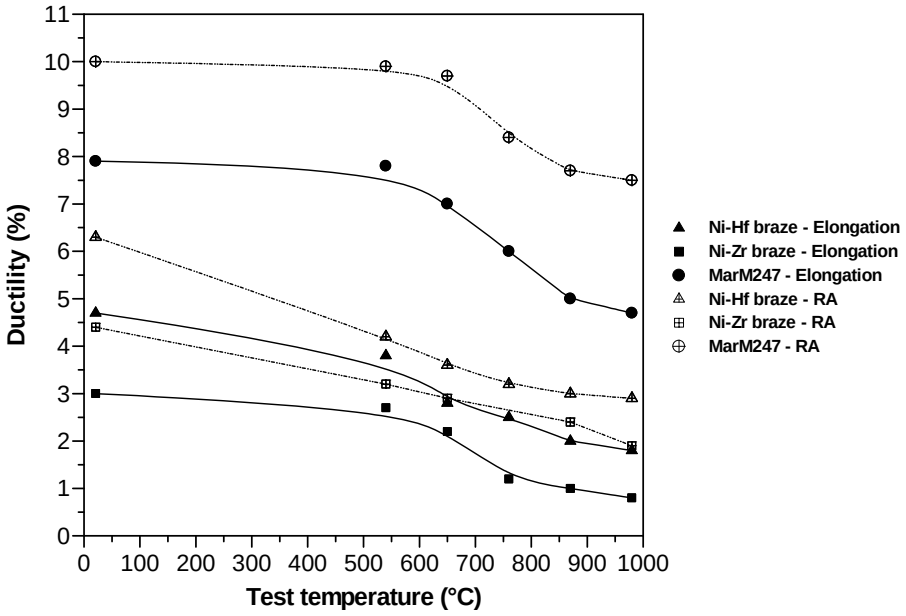

Figure 85 – The ductility of the Ni-Hf and Ni-Zr braze joints and the MarM247 parent metal expressed as % elongation and % reduction in area (RA) as a function of the test temperature (each data point shown represents the average of three tests).

As shown in **Table 12**, the tensile and yield strengths of the Ni-Hf joints at 540°C were 32% and 30%, respectively, of the MarM247 base metal properties, whereas the tensile and yield strengths of the Ni-Zr joints were 55% and 67%, respectively, of those of the MarM247 base metal. The same trend is evident at 650°C, shown in **Table 13**, which indicates that the tensile and yield strengths of the Ni-Hf joints were approximately 33% of the MarM247 base metal properties, and those of the Ni-Zr joints 54% and 64%, respectively, of the MarM247 strength levels. The Ni-Hf joints were therefore considerably weaker than the Ni-Zr joints at 540°C and 650°C. As was the case at room temperature, however, the Ni-Hf joints displayed higher ductility than the Ni-Zr joints. At 540°C, the Ni-Hf joint had approximately 50% of the MarM247 ductility, compared to about 35% for the Ni-Zr joint. At 650°C, the ductility changed to 40% and 32% of the MarM247 ductility for the Ni-Hf and the Ni-Zr joints, respectively.

At higher temperatures, the tensile and yield strengths of the Ni-Hf LPDB joints increased slightly relative to those of the base metal, as shown in **Figure 84** and **Tables 14 to 16** for test temperatures of 760°C, 870°C and 980°C, respectively. The Ni-Hf joint tensile strength increased from 33% of the base metal strength at 760°C, to 37% at 870°C and 39% at 980°C. This trend was not observed for the Ni-Zr joints, with the tensile strength changing from 59% of the base metal strength, to 56% and finally to 52% as the test temperature increased. The yield strength of the Ni-Hf joints changed from 35% of the base metal yield strength at 760°C, to 33% at 870°C and 45% at 980°C. Corresponding yield strength values for the Ni-Zr joint were at 68%, 64% and 79% of the base metal yield strength at 760°C, 870°C and 980°C, respectively. After short processing times (40 minutes), the Ni-Hf joints therefore remained considerably weaker than the Ni-Zr joints as the test temperature increased. The ductility of the Ni-Hf joints was, however, higher than that of the Ni-Zr joints, regardless of test temperature. Ductility values for the Ni-Hf joints changed from 42% of the base metal ductility at 760°C, to 40% at 870°C and 38% at 980°C. Corresponding ductility values for the Ni-Zr joints were approximately 20% of the base metal ductility at 760°C and 870°C, and about 17% at 980°C.

4.4) Conclusions

- A relatively dense, low porosity LPDB joint, with a microstructure consisting of MarM247 powder particles surrounded by Ni-Hf or Ni-Zr braze alloy, formed during processing at 1230°C for 40 minutes. The braze microstructure consisted of γ dendrites and Ni_5Zr or Ni_7Hf_2 intermetallic compound in the form of thick layers surrounding each MarM247 powder particle.

- At all test temperatures (room temperature and at elevated temperatures of 540°C, 650°C, 760°C, 870°C and 980°C), the tensile and yield strengths of the Ni-Zr joints exceeded those of the Ni-Hf joints after short processing times (40 minutes). The tensile and yield strengths of the Ni-Hf joints were typically only about 30 to 40% of those of the MarM247 base metal. For the Ni-Zr joints, the tensile and yield strengths were in the range of 52 to 62% of the MarM247 base metal properties.

- The Ni-Hf joints, however, displayed superior ductility compared to the Ni-Zr joints. Depending on the test temperature, the Ni-Hf joints exhibited ductility on the order of 38 to 60% of that of the MarM247 base metal, whereas the Ni-Zr joints had ductility values in the region of 17 to 40% of the ductility of the MarM247 base metal.

- The ductility of the novel braze alloys containing Hf or Zr as melt point depressant was significantly higher than the ductility of similar joints containing boron as melt point depressant. Boron-containing joints typically exhibit ductility values in the range of 0.5 to 1.0% after short processing times.

- The results described in this chapter were obtained after short processing times of 40 minutes. Longer brazing cycles are frequently used to diffuse melt point depressants into the parent metal and to reduce the occurrence of brittle eutectic phases in the braze joint (as described in Chapter 1). In order to determine whether such an extended brazing cycle will reduce or even eliminate the eutectic films of γ and Ni_5Zr or Ni_7Hf_2 intermetallic compound around the MarM247 powder particles, the brazing time was increased to 4 hours at 1230^{o}C. The results obtained after extended brazing cycle are described in Chapter 5.

CHAPTER 5 - EXPERIMENT 3

CHARACTERIZATION OF THE MICROSTRUCTURE AND MECHANICAL PROPERTIES OF LIQUID PHASE DIFFUSION BONDS USING EUTECTIC Ni-Hf AND Ni-Zr BRAZE ALLOYS AFTER LONGER PROCESSING TIMES (4 HOURS)

5.1) Introduction

The results described in Chapter 4 revealed that a reasonably dense, low porosity LPDB joint, consisting of Ni-Hf or Ni-Zr braze filler metal and MarM247 Ni-base superalloy powder, can be produced using a short brazing cycle (40 minutes at 1230^{o}C). The braze joints consisted of the original MarM247 powder particles encircled by a layer of braze alloy containing γ phase and a Ni_5Zr or Ni_7Hf_2 intermetallic compound.

Experiment 3, described in this chapter, aimed at determining whether a longer brazing time (4 hours at 1230^{o}C) leads to an improvement in the mechanical properties of the brazed joint due to diffusion of the melt point depressant (Hf or Zr) from the braze alloy into the parent metal. If diffusion of the melt point depressant is promoted by the longer brazing cycle, the layers of eutectic braze alloy around the MarM247 powder particles may be reduced in thickness or even eliminated.

5.2) Experimental procedure

In order to study the influence of a longer brazing time, LPDB samples joining In738 parent material were prepared using the procedure described in §4.2. The vacuum brazing cycle, shown below, differed from that used in Experiment 2 (Chapter 4) only in the extended brazing time (4 hours).

1) Ramp up to a temperature of 450^{o}C at a minimum rate of 9^{o}C/minute.
2) Hold at 450^{o}C for 20 minutes to allow the binder to burn off.
3) Ramp up to a temperature of 1150^{o}C at a minimum rate of 9^{o}C/minute.
4) Hold at 1150^{o}C for 20 minutes to allow the samples to stabilize at this temperature.
5) Ramp up to a temperature of 1230^{o}C at a minimum rate of 9^{o}C/minute to melt the Ni-Hf and Ni-Zr braze alloys and to allow the melt to infiltrate the MarM247 powder.
6) Hold at 1230^{o}C for 4 hours.
7) Furnace cool to room temperature.

After exposing the samples to the vacuum LPDB cycle described above, the samples were sectioned, mounted and polished using conventional metallographic practices. The polished metallographic samples were etched with Marble's reagent, and characterized using optical and scanning electron microscopy techniques.

In order to characterize the mechanical properties of the joints, tensile tests were performed at room temperature, and at temperatures of 540^{o}C, 650^{o}C, 760^{o}C, 870^{o}C and 980^{o}C. The tensile samples were prepared by joining MarM247 plate material using the LPDB process and the vacuum brazing cycle described above. After brazing, the tensile test samples were aged at 870^{o}C for 20 hours. The dimensions of the tensile test samples used in this investigation were previously given in **Figure 69**. The LPDB joint was 1.5 mm wide to simulate typical crack widths found in Industrial Gas Turbine (IGT) components, and was located in the centre of the sample gauge length.

5.3) Results and discussion

5.3.1 Microstructural investigation:

The microstructure of the Ni-Hf LPDB joint processed at 1230°C for 4 hours is shown in **Figures 86 to 89.** The joint consists of the original MarM247 powder particles, separated by layers of Ni-Hf braze alloy. It is evident from **Figures 87 and 88** that the layers of γ and Ni_7Hf_2 intermetallic compound between the MarM247 powder particles are finer and less continuous (compared with those shown in **Figures 72 and 73** for a brazing time of 40 minutes). This supports the premise stated in §5.1 that an extended brazing cycle promotes the diffusion of the melt point depressant (Hf) into the parent metal and minimizes the occurrence of intermetallic-containing eutectic component in the braze. This should lead to an improvement in mechanical properties.

The microstructure of the LPDB joint produced using MarM247 powder and Ni-Zr braze paste is shown in **Figures 90 to 93** at various magnifications. The original MarM247 powder particles are evident as the lighter, more equiaxed component, while the darker regions consist of Ni-Zr braze alloy. The braze alloy contains γ dendrites and Ni_5Zr intermetallic compound, but the layers of braze metal around each MarM247 particle appear less continuous and considerably finer than those observed after processing for 40 minutes at 1230°C (**Figures 79 to 81**).

The islands of braze alloy retained between the MarM247 particles resemble the intergranular carbides often observed in Ni-base superalloys (see **Figure 2**). The structures shown in **Figures 86 to 93** can be viewed as consisting of a mixture of fine and coarse-grained material, dispersed with intergranular γ and Ni_7Hf_2 or Ni_5Zr compounds. It is hoped that the mixture of coarse and fine grains within the braze joint will ensure a good combination of high tensile strength (promoted by a fine grain size) and good creep rupture strength (promoted by a coarse grain structure).

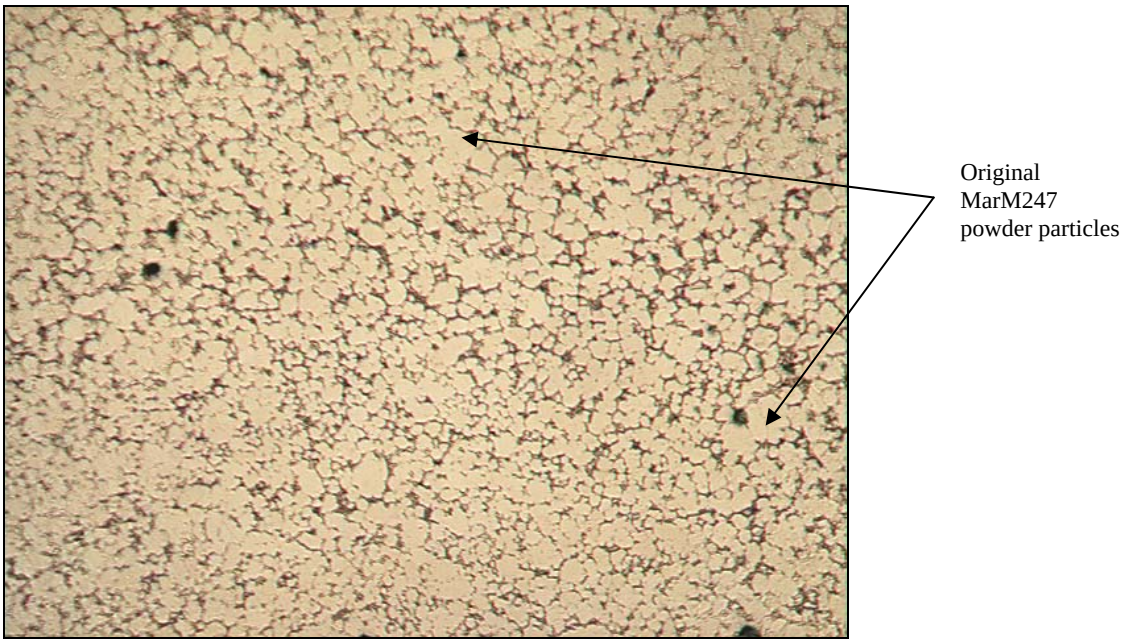

Figure 86 - Ni-Hf braze dispersed between MarM247 powder particles after brazing at 1230°C for 4 hours. Magnification: 50X.

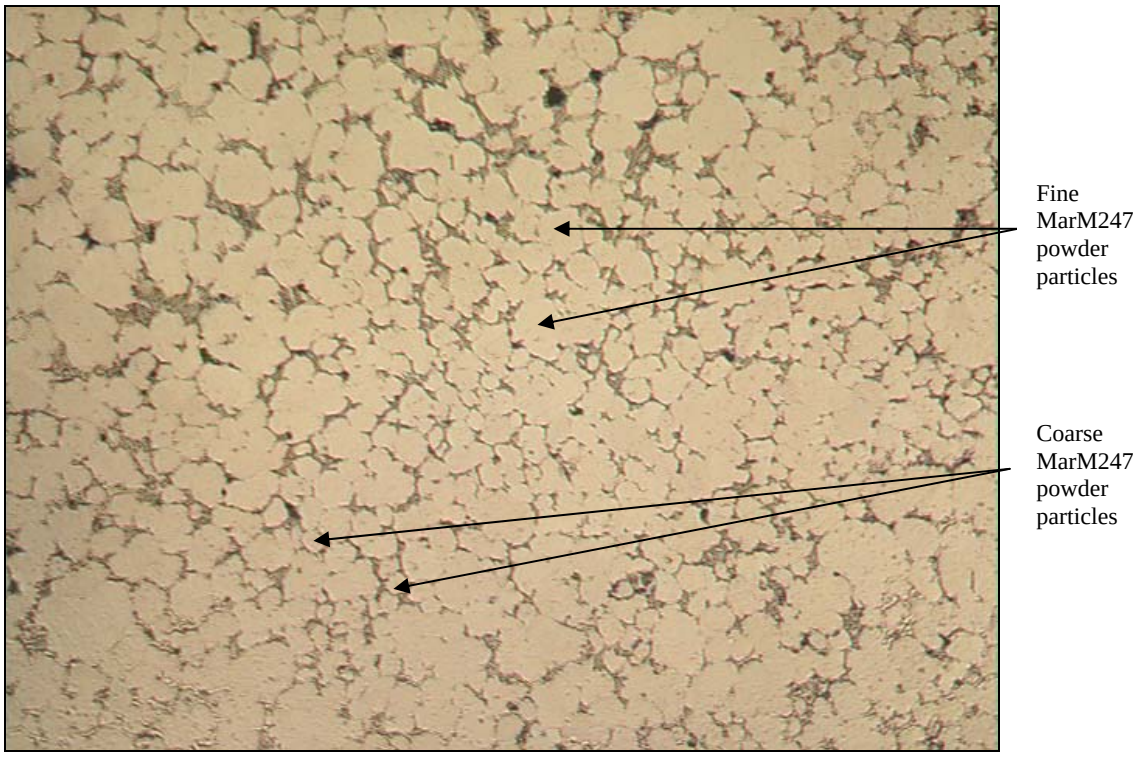

Figure 87 - Ni-Hf braze dispersed between MarM247 powder particles after brazing at 1230°C for 4 hours. Magnification: 100X.

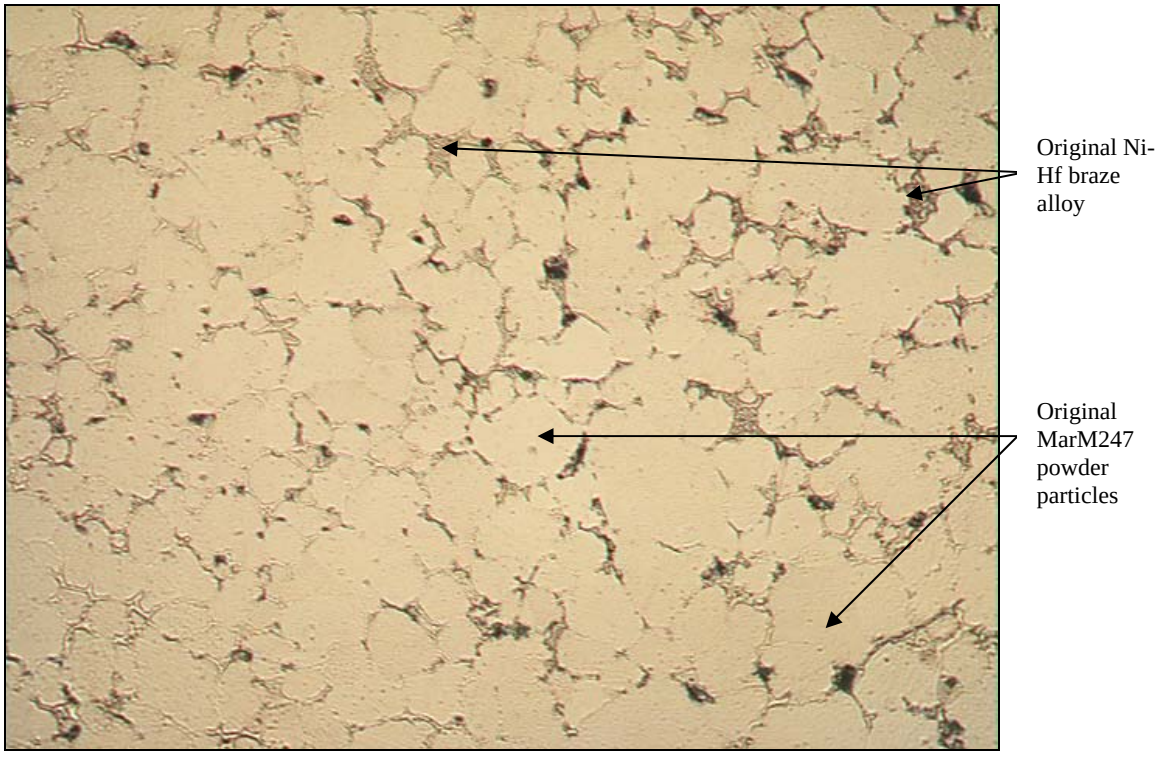

Figure 88 - Ni-Hf braze dispersed between MarM247 powder particles after brazing at 1230°C for 4 hours. Magnification: 200X.

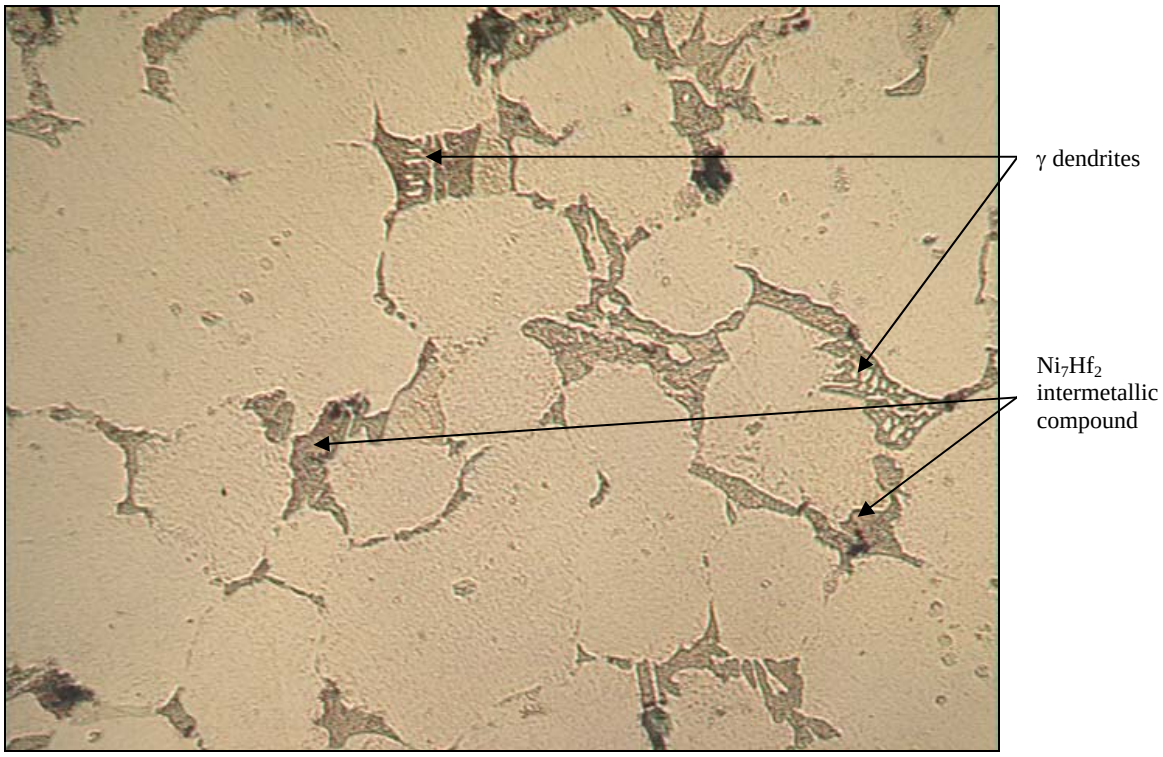

Figure 89 - Ni-Hf braze dispersed between MarM247 powder particles after brazing at 1230°C for 4 hours. Magnification: 500X.

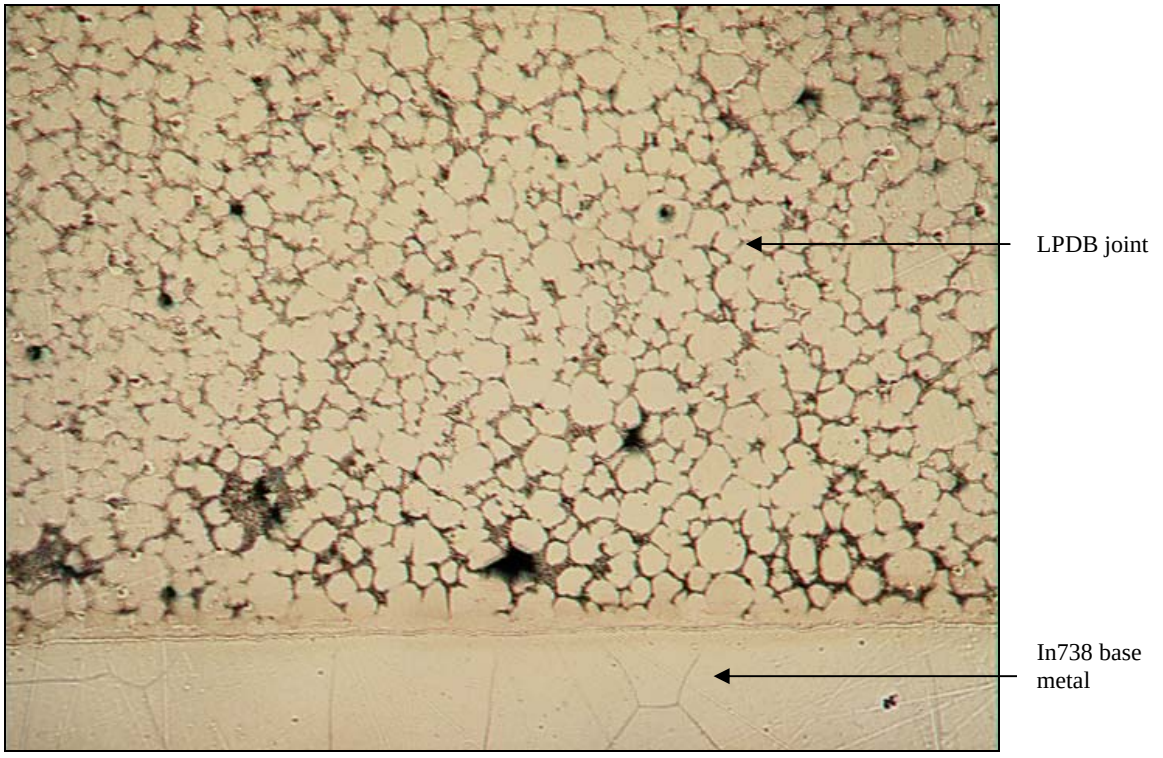

Figure 90 - Ni-Zr braze dispersed between MarM247 powder particles after brazing at 1230°C for 4 hours. Magnification: 50X.

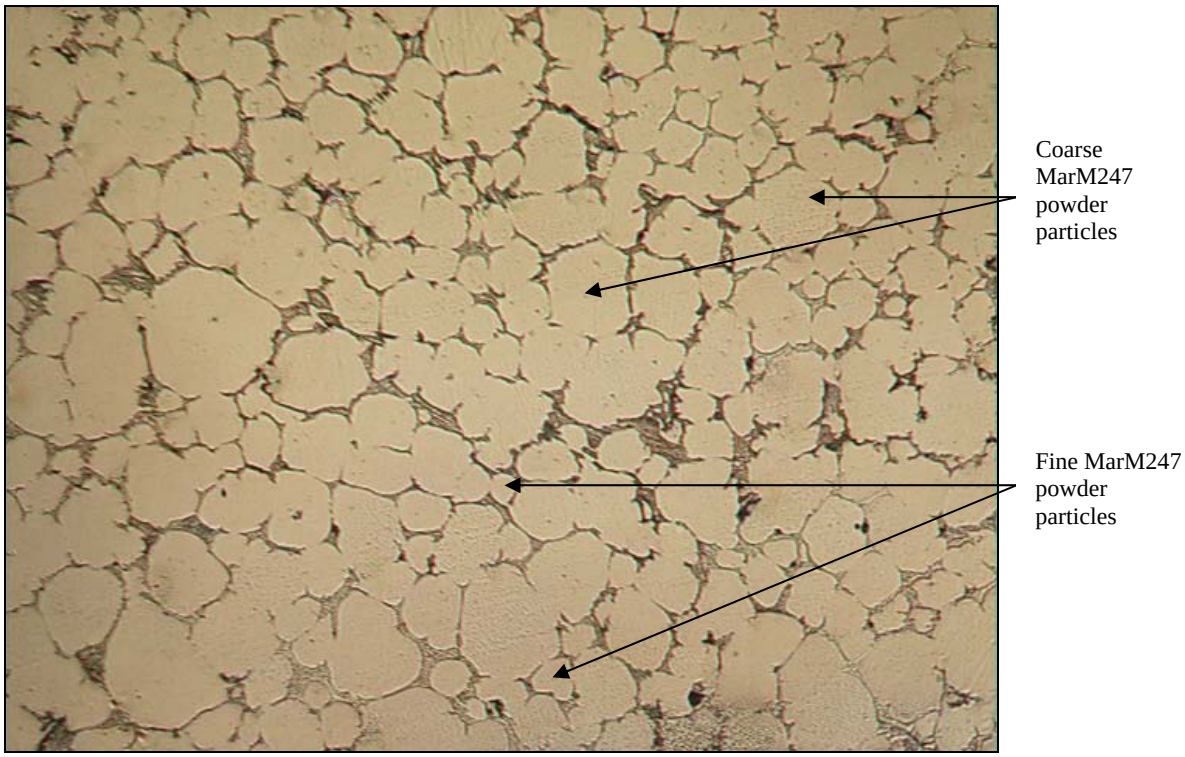

Figure 91 - Ni-Zr braze dispersed between MarM247 powder particles after brazing at 1230°C for 4 hours. Magnification: 100X.

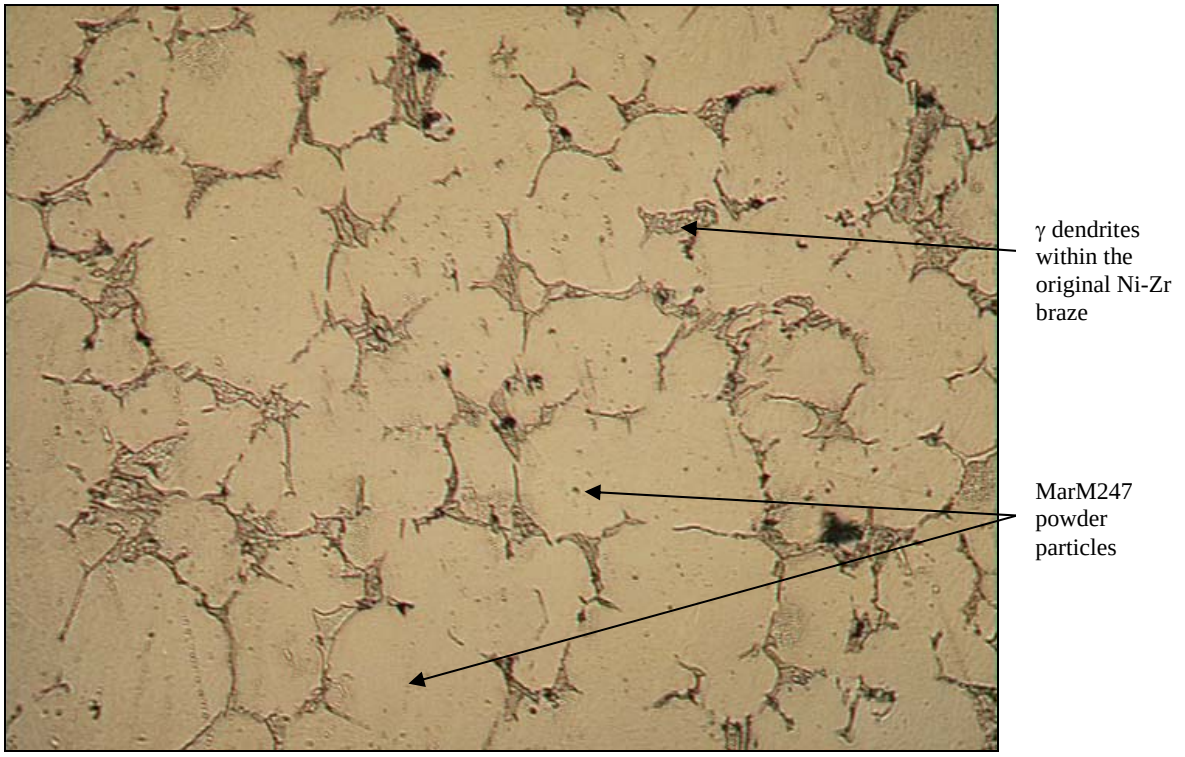

Figure 92 - Ni-Zr braze dispersed between MarM247 powder particles after brazing at 1230°C for 4 hours. Magnification: 200X.

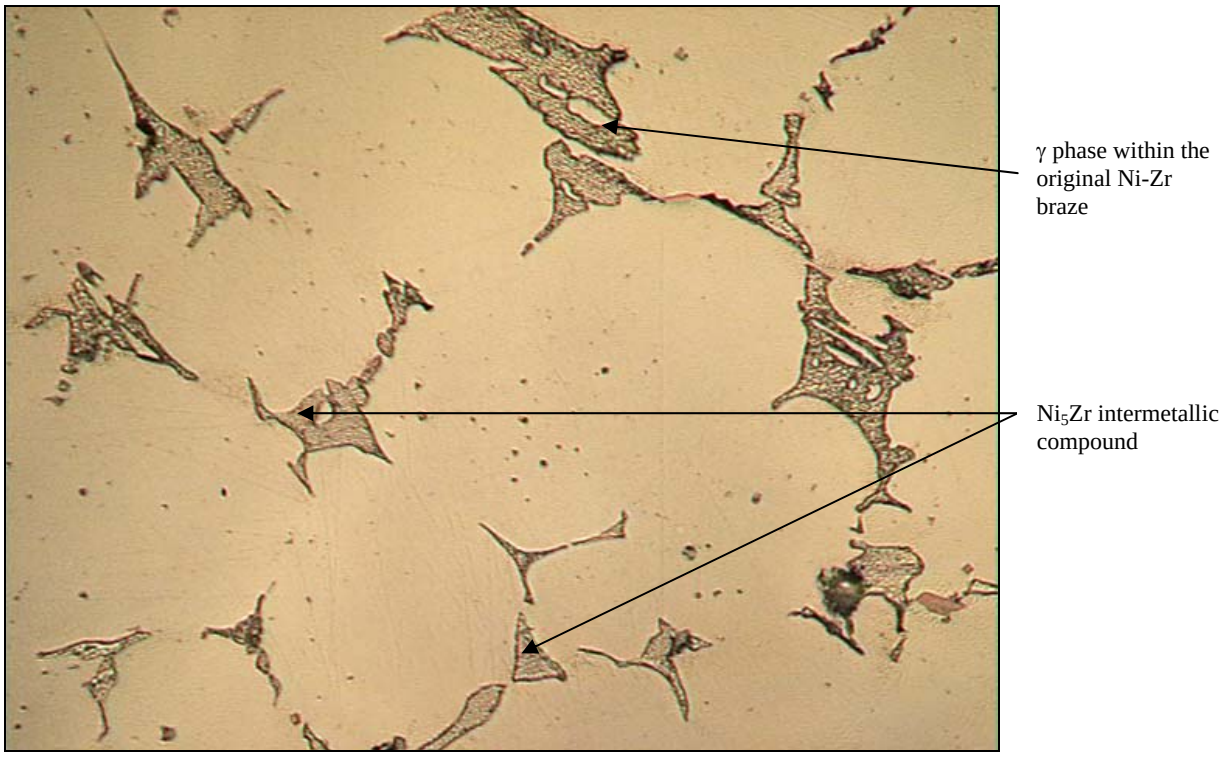

Figure 93 - Ni-Zr braze dispersed between MarM247 powder particles after brazing at 1230°C for 4 hours. Magnification: 500X.

Figure 94 displays a SEM micrograph of the MarM247/Ni-Hf joint brazed at 1230°C for 4 hours. Two phases, highlighted by the arrows in **Figure 94,** were analyzed using the SEM-EDS technique. The phase arbitrarily labelled "grain boundary particle" was identified as γ dendrites (with a composition of 75.27Ni-6.26Co-6.88Cr-3.67Al-2.29W-2.22Fe-1.93Mo-0.73Ti-0.74Zr) (wt. %). The second phase, arbitrarily labelled "grain boundary film", had a composition of 49.50Ni-46.56Hf-1.36W-2.01Co-0.38Cr-0.19Ti (wt.%). This phase was provisionally identified as the Ni_7Hf_2 intermetallic phase, with small amounts of W, Co, Cr and Ti in solution.

A SEM micrograph of the MarM247/Ni-Zr joint after brazing at 1230°C for 4 hours is shown in **Figure 95**. SEM-EDS analysis revealed that the phase arbitrarily labelled "grain boundary particle" consisted of 79.54Ni-5.90Co-5.34Cr-3.98Al-1.81W-11.11Fe-0.85Mo-0.64Ti-0.83Zr (wt.%). On the basis of this composition, the "grain boundary particle" phase was identified as γ. The second phase was arbitrarily labelled "grain boundary film", and consisted of 71.35Ni-24.47Zr-0.70W-2.28Co-0.61Cr-0.16Mo-0.43Al (wt.%). This phase was identified as the Ni_5Zr intermetallic phase, with some W, Co, Cr, Mo and Al in solution.

5.3.2 Tensile test results:

The results of tensile tests performed at various temperatures are shown in **Tables 17 to 22** and presented graphically in **Figures 96 to 99**. The values shown represent the average of three tests.

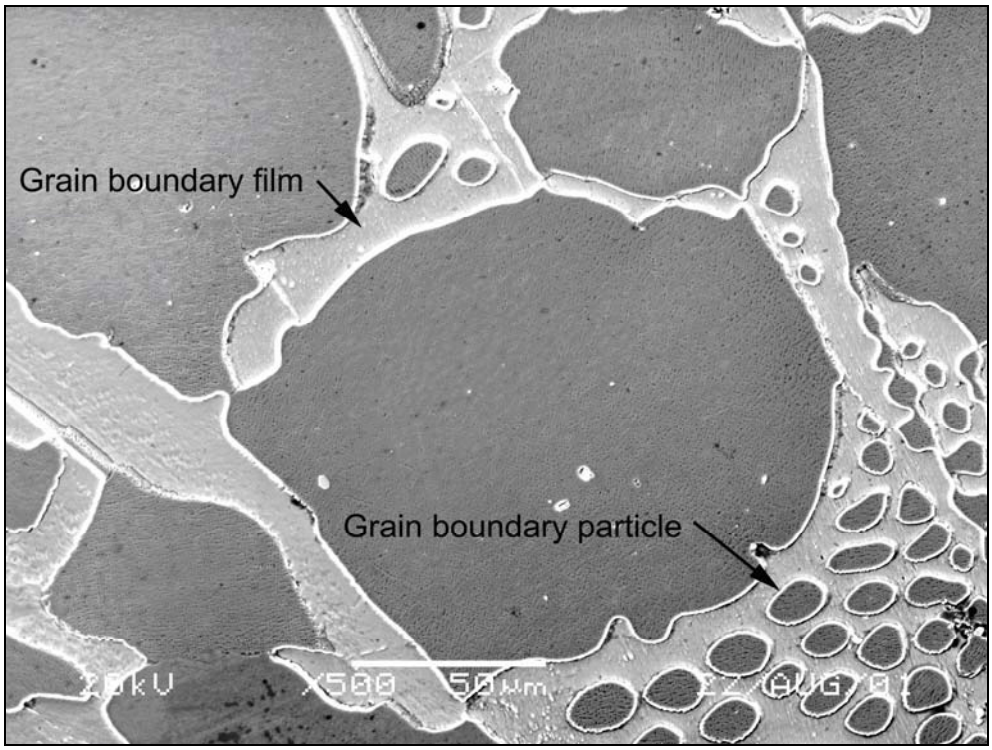

Figure 94 – SEM micrograph of the Ni-Hf braze, showing the phases identified as γ (labelled "grain boundary particle") and Ni_7Hf_2 (labelled "grain boundary film").

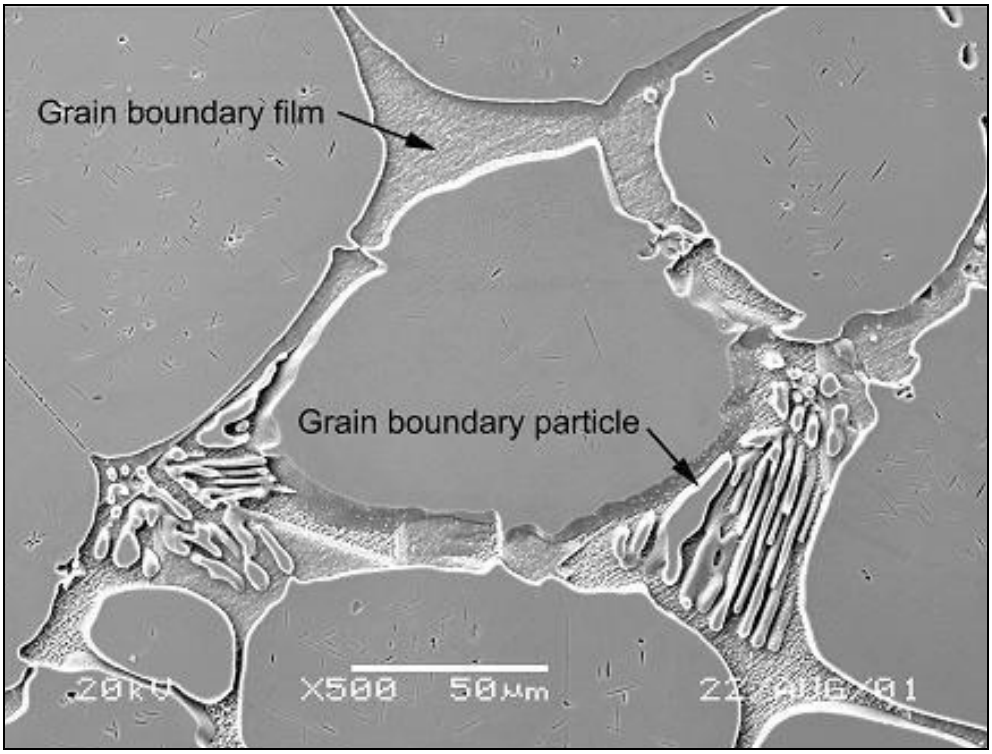

Figure 95 – SEM micrograph of the Ni-Zr braze, showing the phases identified as γ (labelled "grain boundary particle") and Ni_5Zr (labelled "grain boundary film").

Table 17 – Joint tensile properties measured at 21°C.

Tensile properties	**Ni-Hf joints** 1230°C for 40 min.	**Ni-Hf joints** 1230°C for 4 hours	**Ni-Zr joints** 1230°C for 40 min.	**Ni-Zr joints** 1230°C for 4 hours	**MarM247 Base metal**
Tensile strength	323 MPa (46.8 ksi)	344 MPa (49.8 ksi)	557 MPa (80.7 ksi)	564 MPa (81.7 ksi)	960 MPa (139 ksi)
Yield strength	239 MPa (34.7 ksi)	302 MPa (43.8 ksi)	505 MPa (73.2 ksi)	511 MPa (74.0 ksi)	800 MPa (116 ksi)
Elongation (%)	4.7	2.7	3.0	3.0	7.9
Reduction in area (%)	6.3	3.9	4.4	4.5	10.0

Table 18 – Joint tensile properties measured at 540°C.

Tensile properties	**Ni-Hf joints** 1230°C for 40 min.	**Ni-Hf joints** 1230°C for 4 hours	**Ni-Zr joints** 1230°C for 40 min.	**Ni-Zr joints** 1230°C for 4 hours	**MarM247 Base metal**
Tensile strength	328 MPa (47.6 ksi)	406 MPa (58.9 ksi)	619 MPa (89.7 ksi)	625 MPa (90.6 ksi)	1014 MPa (147 ksi)
Yield strength	243 MPa (35.2 ksi)	329 MPa (47.7 ksi)	539 MPa (78.1 ksi)	556 MPa (80.6 ksi)	801 MPa (116 ksi)
Elongation (%)	3.8	3.0	2.7	2.8	7.9
Reduction in area (%)	4.2	3.8	3.2	3.4	10.0

Table 19 – Joint tensile properties measured at 650°C.

Tensile properties	**Ni-Hf joints** 1230°C for 40 min.	**Ni-Hf joints** 1230°C for 4 hours	**Ni-Zr joints** 1230°C for 40 min.	**Ni-Zr joints** 1230°C for 4 hours	**MarM247 Base metal**
Tensile strength	343 MPa (49.7 ksi)	408 MPa (59.1 ksi)	562 MPa (81.4 ksi)	569 MPa (82.5 ksi)	1040 MPa (151 ksi)
Yield strength	265 MPa (38.4 ksi)	308 MPa (44.7 ksi)	513 MPa (74.4 ksi)	501 MPa (72.6 ksi)	805 MPa (117 ksi)
Elongation (%)	2.8	3.1	2.2	2.3	7.0
Reduction in area (%)	3.6	3.8	2.9	2.9	9.7

Table 20 – Joint tensile properties measured at 760°C.

Tensile properties	**Ni-Hf joints** 1230°C for 40 min.	**Ni-Hf joints** 1230°C for 4 hours	**Ni-Zr joints** 1230°C for 40 min.	**Ni-Zr joints** 1230°C for 4 hours	**MarM247 Base metal**
Tensile strength	333 MPa (48.3 ksi)	464 MPa (67.2 ksi)	593 MPa (85.9 ksi)	602 MPa (87.3 ksi)	1000 MPa (145 ksi)
Yield strength	282 MPa (40.8 ksi)	380 MPa (55.1 ksi)	553 MPa (80.1 ksi)	524 MPa (75.9 ksi)	815 MPa (118 ksi)
Elongation (%)	2.5	2.9	1.2	2.2	6.0
Reduction in area (%)	3.2	3.0	5.9	4.3	8.4

Table 21 – Joint tensile properties measured at 870°C.

Tensile properties	**Ni-Hf joints** 1230°C for 40 min.	**Ni-Hf joints** 1230°C for 4 hours	**Ni-Zr joints** 1230°C for 40 min.	**Ni-Zr joints** 1230°C for 4 hours	**MarM247 Base metal**
Tensile strength	289 MPa (41.9 ksi)	342 MPa (49.6 ksi)	444 MPa (64.4 ksi)	480 MPa (69.6 ksi)	790 MPa (115 ksi)
Yield strength	211 MPa (30.5 ksi)	277 MPa (40.1 ksi)	414 MPa (60.0 ksi)	404 MPa (58.6 ksi)	650 MPa (94 ksi)
Elongation (%)	2.0	2.2	1.0	2.1	5.0
Reduction in area (%)	3.0	3.2	2.4	3.1	7.7

Table 22 – Joint tensile properties measured at 980°C.

Tensile properties	**Ni-Hf joints** 1230°C for 40 min.	**Ni-Hf joints** 1230°C for 4 hours	**Ni-Zr joints** 1230°C for 40 min.	**Ni-Zr joints** 1230°C for 4 hours	**MarM247 Base metal**
Tensile strength	195 MPa (28.3 ksi)	266 MPa (38.6 ksi)	261 MPa (37.8 ksi)	308 MPa (44.7 ksi)	506 MPa (73 ksi)
Yield strength	141 MPa (20.4 ksi)	206 MPa (29.9 ksi)	245 MPa (35.5 ksi)	214 MPa (31.0 ksi)	312 MPa (45 ksi)
Elongation (%)	1.8	2.7	0.8	3.1	4.7
Reduction in area (%)	2.9	3.1	1.9	6.2	7.5

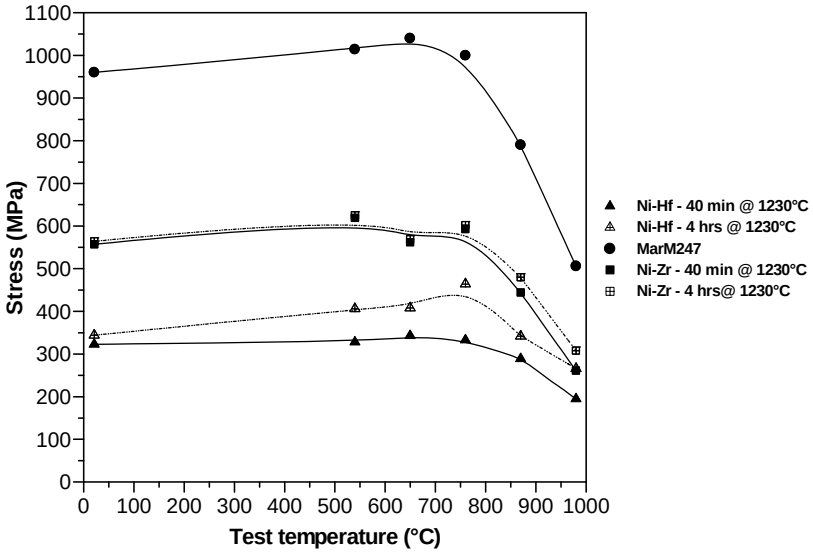

Figure 96 – The tensile strength (UTS) of the Ni-Hf and Ni-Zr braze joints and the MarM247 parent metal as a function of the test temperature and braze time (each data point shown represents the average of three tests).

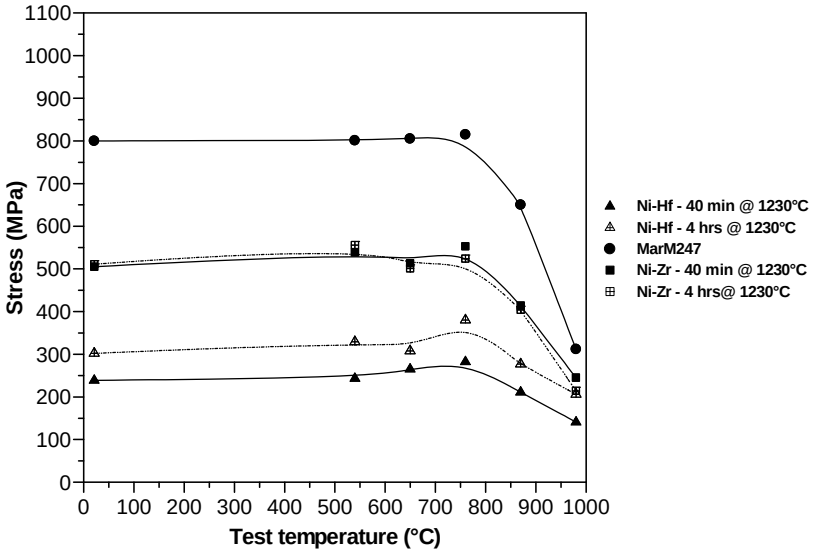

Figure 97 – The yield stress of the Ni-Hf and Ni-Zr braze joints and the MarM247 parent metal as a function of the test temperature and braze time (each data point shown represents the average of three tests).

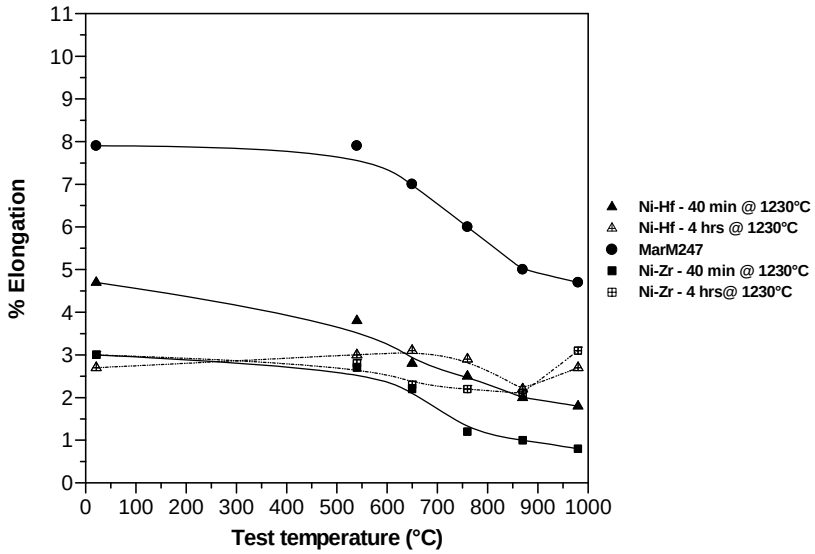

Figure 98 – The % elongation measured for the Ni-Hf and Ni-Zr braze joints and the MarM247 parent metal as a function of the test temperature and braze time (each data point shown represents the average of three tests).

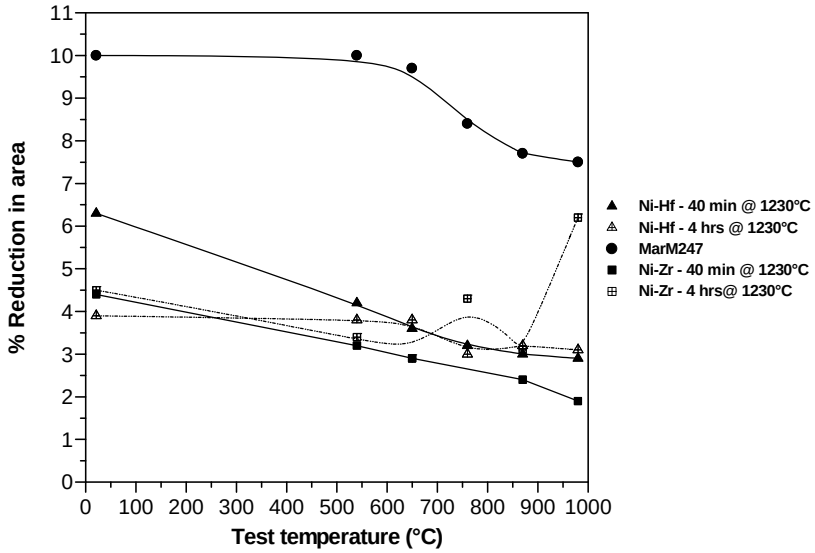

Figure 99 – The % reduction in area measured for the Ni-Hf and Ni-Zr braze joints and the MarM247 parent metal as a function of the test temperature and braze time (each data point shown represents the average of three tests).

As shown in **Figures 96 and 97**, the tensile and yield strengths of the Ni-Hf braze alloy were improved considerably over the entire range of tensile test temperatures by increasing the brazing time. The measured joint tensile strength values ranged from approximately 36% of the base metal tensile strength at room temperature, to about 53% at a test temperature of 980°C. The measured yield strength values ranged from about 38% (at room temperature) to 56% of the base metal yield strength (at 980°C). This suggests that the longer braze cycle facilitated the diffusion of the melt point depressant into the parent metal (as suggested by **Figures 87 to 89**), reducing the amount of brittle intermetallic compound in the joint and allowing the mechanical properties of the braze joint to approach those of the MarM247

superalloy powder. The longer braze time reduced the ductility of the joint at lower test temperatures, but at higher temperatures the ductility was improved (**Figures 98 and 99**).

The tensile and yield strength values of the Ni-Zr braze joint exceeded those of the Ni-Hf joint at all test temperatures, attaining levels of approximately 60% of the base metal tensile strength, and up to 70% of the base metal yield strength after brazing for 4 hours (**Figures 96 and 97**). The longer braze time, however, did not improve the joint strength to any significant extent. A significant improvement in ductility was, however, evident after 4 hours at 1230°C, particularly at higher test temperatures. The measured joint ductility ranged from about 38% of the base metal ductility at room temperature, to approximately 74% at 980°C (**Figures 98 and 99**).

5.4) Conclusions

- A relatively dense, low porosity LPDB joint, with a microstructure consisting of MarM247 powder particles surrounded by Ni-Hf or Ni-Zr braze alloy, formed during processing at 1230^{o}C for 4 hours. The braze microstructure consisted of γ dendrites and Ni_5Zr or Ni_7Hf_2 intermetallic compound.

- Brazing at 1230°C for 4 hours, compared to 40 minutes, decreased the amount of Ni_5Zr/Ni_7Hf_2 intermetallic compound, and reduced the thickness of the layers of braze alloy surrounding the MarM247 powder particles. The regions of braze alloy between the powder particles appeared less continuous after 4 hours, and in many areas only isolated γ dendrites and Ni_5Zr/Ni_7Hf_2 phases existed between the superalloy particles.

- At all test temperatures, the tensile and yield strength values of the Ni-Zr joints exceeded those of the Ni-Hf joints. The measured Ni-Hf joint strength ranged from approximately 36% of the base metal tensile strength and 38% of the yield strength at room temperature, to about 53% of the tensile strength and 56% of the yield strength at a test temperature of 980°C. The Ni-Zr joint attained strength levels of approximately 60% of the base metal tensile strength, and up to 70% of the base metal yield strength after a braze time of 4 hours.

- A longer braze cycle (4 hours compared to 40 minutes at 1230°C) significantly improved the strength of the Ni-Hf joint, but had little effect on the strength of the Ni-Zr joint. Both joints exhibited a significant improvement in ductility after the extended braze cycle, particularly at higher test temperatures.

- The ductility of the novel braze alloys containing Hf or Zr as melt point depressant was significantly higher than the ductility of similar joints containing boron as melt point depressant. Boron-containing joints typically exhibit ductility values in the range of 0.5 to 1.0% after short processing times.

- The results described in this chapter were obtained after processing times of 4 hours. In order to determine whether an even longer brazing cycle will further reduce or even eliminate the eutectic films of γ and Ni_5Zr or Ni_7Hf_2 intermetallic compound around the MarM247 powder particles, the brazing time was increased to 12 hours at 1230^{o}C. The results of this experiment are described in Chapter 6.

CHAPTER 6 - EXPERIMENT 4

CHARACTERIZATION OF THE MICROSTRUCTURE AND MECHANICAL PROPERTIES OF LIQUID PHASE DIFFUSION BONDS USING EUTECTIC Ni-Hf AND Ni-Zr BRAZE ALLOYS AFTER EXTENDED BRAZING TIMES (12 HOURS)

6.1) Introduction

The results described in Chapter 5 revealed that a reasonably dense, low porosity LPDB joint, consisting of Ni-Hf or Ni-Zr braze filler metal and MarM247 Ni-base superalloy powder, can be produced by brazing for 4 hours at 1230°C. After processing the braze joints consisted of the original MarM247 powder particles surrounded by a layer of γ phase and Ni_5Zr or Ni_7Hf_2 intermetallic compound. Increasing the braze time from 40 minutes to 4 hours reduced the thickness of the braze layer around the MarM247 powder particles and increased the tensile and yield strengths of the Ni-Hf braze joint at all test temperatures. The strength of the Ni-Zr joint was not improved significantly by extending the braze cycle, but the ductility of both braze joints was improved, particularly at higher test temperatures. These results suggest that the extended braze cycle promoted the diffusion of the melt point depressants from the braze metal into the parent plate, partially decomposing the brittle eutectic phases within the braze joints, and resulting in improved mechanical properties.

Since extending the braze cycle from 40 minutes to 4 hours yielded promising results, Experiment 4 aimed at determining whether an even longer braze cycle (12 hours at 1230°C, followed by solution annealing at the same temperature for an additional 4 hours) promotes further decomposition of the layers of γ and Ni_7Hf_2/Ni_5Zr surrounding the MarM247 powder particles. Creep rupture tests were also performed at various stress levels at three elevated temperatures in order to obtain preliminary creep/stress rupture properties for the MarM247/Ni-Zr and MarM247/Ni-Hf braze formulations.

6.2) Experimental procedure

Liquid phase diffusion bonding was used to join In738 parent material using the eutectic Ni-Hf and Ni-Zr braze alloys described in earlier chapters. The braze samples were prepared using the procedure presented in §4.2. The vacuum brazing cycle, shown below, differed from those described in Chapters 4 and 5 only in the extended brazing time (12 hours) used.

1) Ramp up to a temperature of 450°C at a minimum rate of 9°C/minute.
2) Hold at 450°C for 20 minutes to allow the binder to burn off.
3) Ramp up to a temperature of 1150°C at a minimum rate of 9°C/minute.
4) Hold at 1150°C for 20 minutes to allow the samples to stabilize at this temperature.
5) Ramp up to a temperature of 1230°C at a minimum rate of 9°C/minute to melt the Ni-Hf and Ni-Zr braze alloys and to allow the melt to infiltrate the MarM247 powder.
6) Hold at 1230°C for 12 hours.
7) Furnace cool to room temperature.

After joining the samples using the LPDB cycle described above, the brazed samples were placed in a production vacuum furnace equipped with quenching facilities in order to solution anneal the joints. Gas quenching, using 2 bar argon pressure, was utilized on completion of

the solution annealing cycle. A conventional vacuum solution heat treatment cycle, similar to that applied in industry to MarM247 Siemens Westinghouse blades operating in W501F turbine engines, was applied. The solution heat treatment used in this experiment was as follows:

1) Ramp up to a temperature of 1230°C at a minimum rate of 14°C per minute.
2) Hold at 1230°C for 4 hours.
3) Quench to room temperature at a rate of 50°C per minute.

After exposing the plates to the vacuum LPDB and solution heat treatment cycles described above, samples were sectioned, mounted and polished using conventional metallographic techniques. The polished metallographic samples were then etched with Marble's reagent, and characterized using optical and scanning electron microscopy.

In order to obtain preliminary creep/stress rupture properties for the novel braze formulations, creep rupture tests were performed at three temperatures: 845°C, 900°C and 980°C. Samples were subjected to three different applied stress levels at each test temperature, as indicated in **Table 23**. The creep rupture test samples were prepared by joining In738 plate material using the LPDB process and the vacuum brazing and solution heat treatment cycles described above. The dimensions of the test specimens used in this investigation were identical to those given in **Figure 69**. The joint was located in the centre of the gauge length and the joint gap was maintained at 1.5 mm to simulate typical crack widths found in Industrial Gas Turbine (IGT) components.

Table 23 - Creep rupture test conditions.

Test temperature	Stress level #1	Stress level #2	Stress level #3
845°C	345 MPa (50 ksi)	276 MPa (40 ksi)	228 MPa (33 ksi)
900°C	242 MPa (35 ksi)	186 MPa (27 ksi)	152 MPa (22 ksi)
980°C	138 MPa (20 ksi)	104 MPa (15 ksi)	76 MPa (11 ksi)

The metallographic examination and creep rupture tests were performed on samples in the solution annealed condition. In industry, In738 turbine components normally receive an aging heat treatment after solution annealing – typically at a temperature of approximately 1120°C for 2 hours, followed by an additional 24 hours at 845°C. Not aging the samples used in this experiment was an oversight on the author's part due to a misunderstanding. Even though the samples were not aged, the results presented in this chapter still allow a comparison between the Ni-Zr and Ni-Hf braze compositions. It must be borne in mind, however, that since the samples were tested in the solution heat treated condition without any aging, the material is likely to be softer and to exhibit enhanced ductility and reduced creep rupture strength compared to fully aged specimens.

6.3) Results and discussion

6.3.1 Microstructural investigation:

The microstructure of the Ni-Hf LPDB joint processed at 1230°C for 12 hours, followed by solution annealing, is shown in **Figures 100 to 103.** The joint consists of the original MarM247 powder particles, surrounded by layers of Ni-Hf braze alloy. This microstructure resembles the microstructure of the Ni-Hf joint processed at 1230°C for 4 hours, shown in

Figures 86 to 89. The layers of γ and Ni_7Hf_2 between the MarM247 powder particles appear finer and less continuous (compared with those shown in **Figures 72 and 73** for a brazing time of 40 minutes), supporting the conclusion that an extended brazing cycle promotes the diffusion of the melt point depressant (Hf) into the parent metal and minimizes the amount of brittle intermetallic compound in the braze.

The microstructure of the LPDB joint produced with MarM247 powder and Ni-Zr braze paste is shown in **Figures 104 to 107** at various magnifications. The original MarM247 powder particles are evident as the lighter, more equiaxed component, while the darker regions consist of retained eutectic Ni-Zr braze alloy. The microstructure of the MarM247/Ni-Zr joint processed at 1230°C for 12 hours, followed by solution heat treatment, resembles the microstructure shown in **Figures 90 to 93** for a braze cycle of 4 hours. The braze alloy contains γ dendrites and Ni_5Zr intermetallic compound, but the layers of braze metal around each MarM247 particle are less continuous and significantly finer than those observed after processing for 40 minutes at 1230°C (**Figures 79 to 81**). The islands of braze alloy retained between the MarM247 powder particles resemble the intergranular carbides often observed in Ni-base superalloys (see **Figure 2**). The structures shown in **Figures 100 to 107** can be viewed as consisting of a mixture of fine and coarse-grained superalloy material, dispersed with intergranular γ and Ni_7Hf_2/Ni_5Zr intermetallic compound. It is hoped that the mixture of coarse and fine grains within the braze joint will ensure a good combination of high tensile strength (promoted by a fine grain size) and good creep rupture strength (promoted by a coarse grain structure).

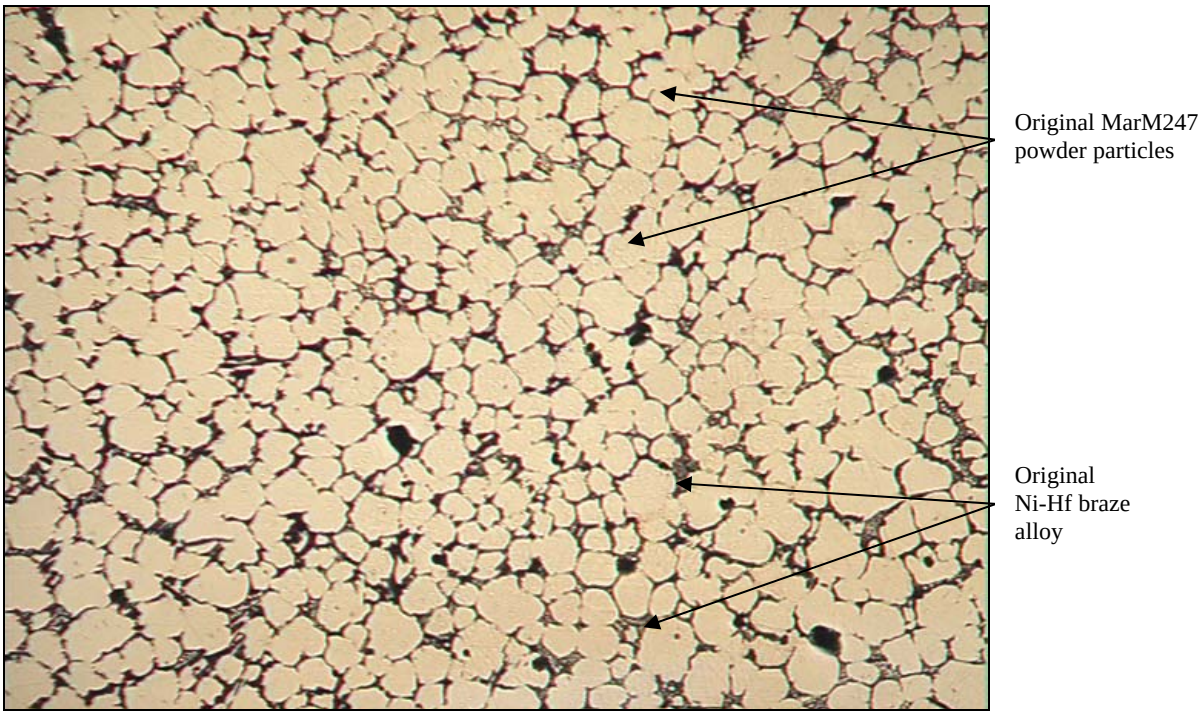

Figure 100 - Ni-Hf braze dispersed between MarM247 powder particles after brazing at 1230°C for 12 hours, followed by solution heat treatment at 1230°C for 4 hours and quenching. Magnification: 50X.

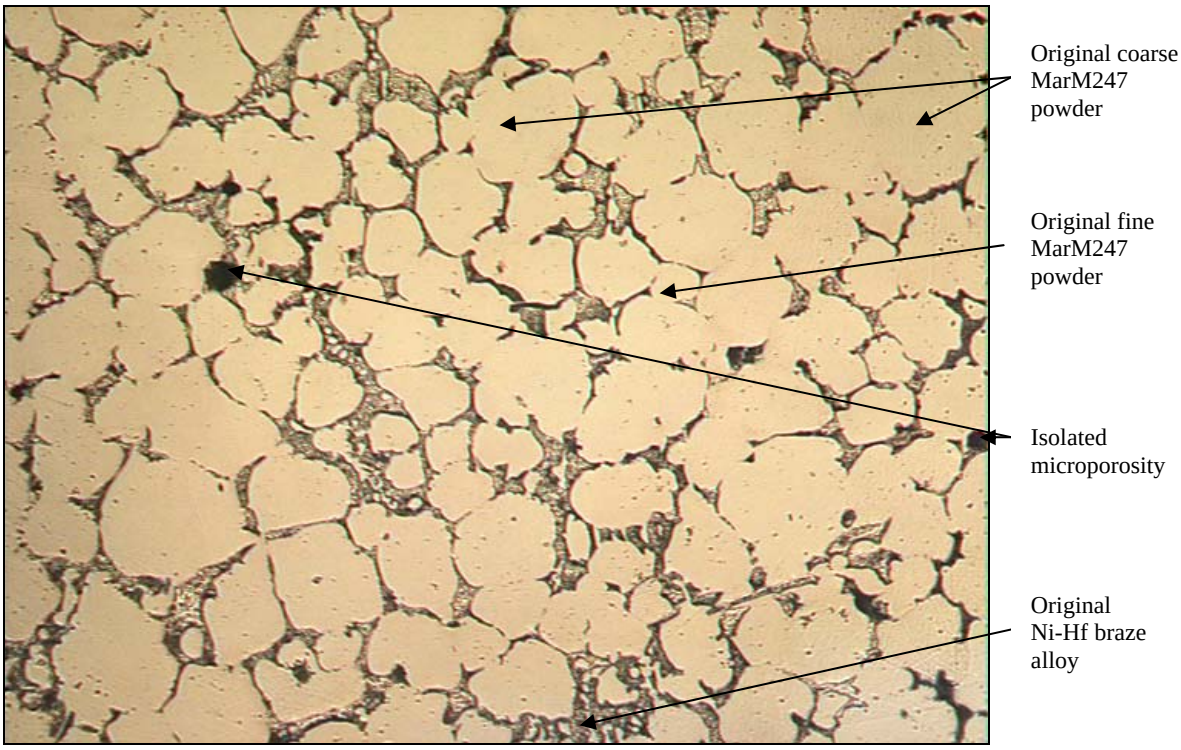

Figure 101 - Ni-Hf braze dispersed between MarM247 powder particles after brazing at 1230°C for 12 hours, followed by solution heat treatment at 1230°C for 4 hours and quenching. Magnification: 100X.

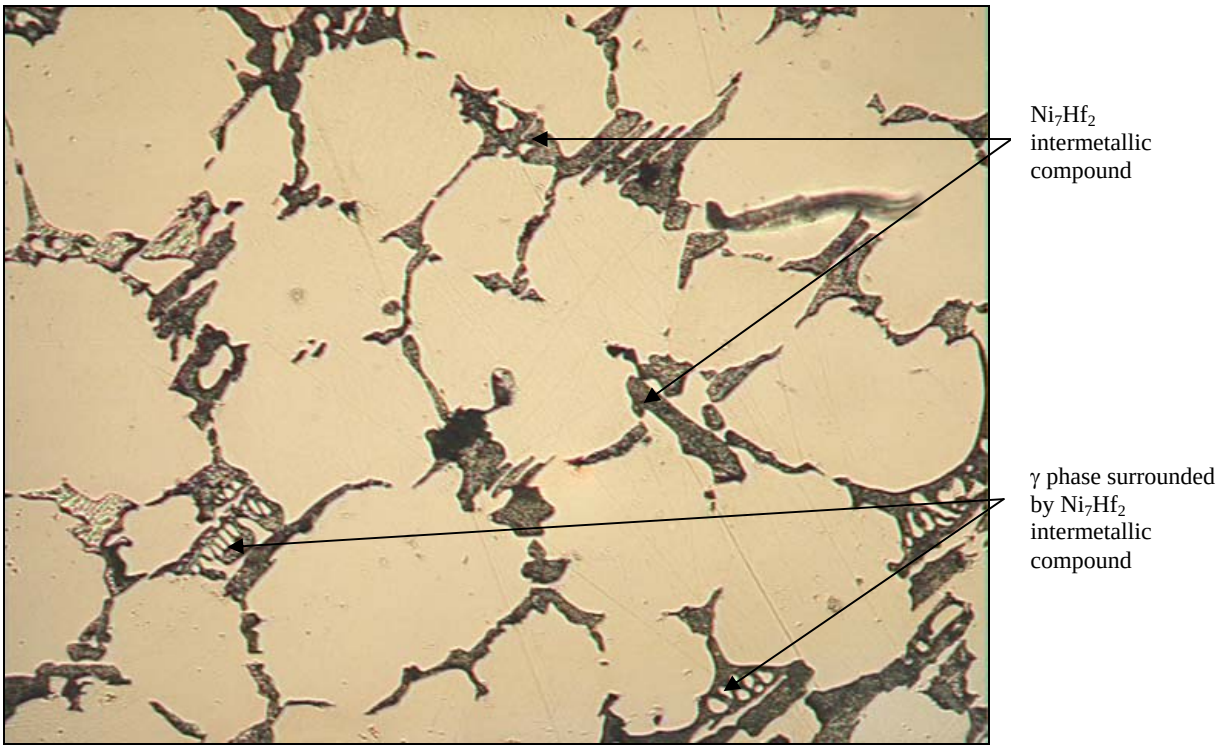

Figure 102 - Ni-Hf braze dispersed between MarM247 powder particles after brazing at 1230°C for 12 hours, followed by solution heat treatment at 1230°C for 4 hours and quenching. Magnification: 200X.

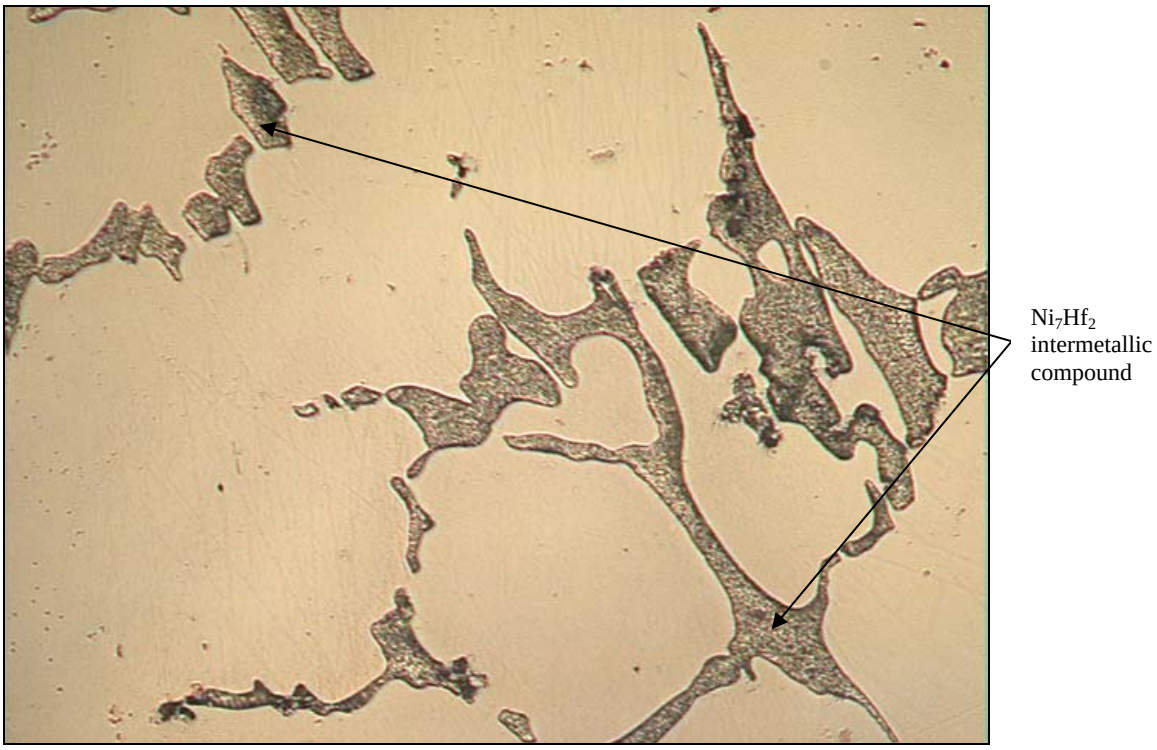

Figure 103 - Ni-Hf braze dispersed between MarM247 powder particles after brazing at 1230°C for 12 hours, followed by solution heat treatment at 1230°C for 4 hours and quenching. Magnification: 500X.

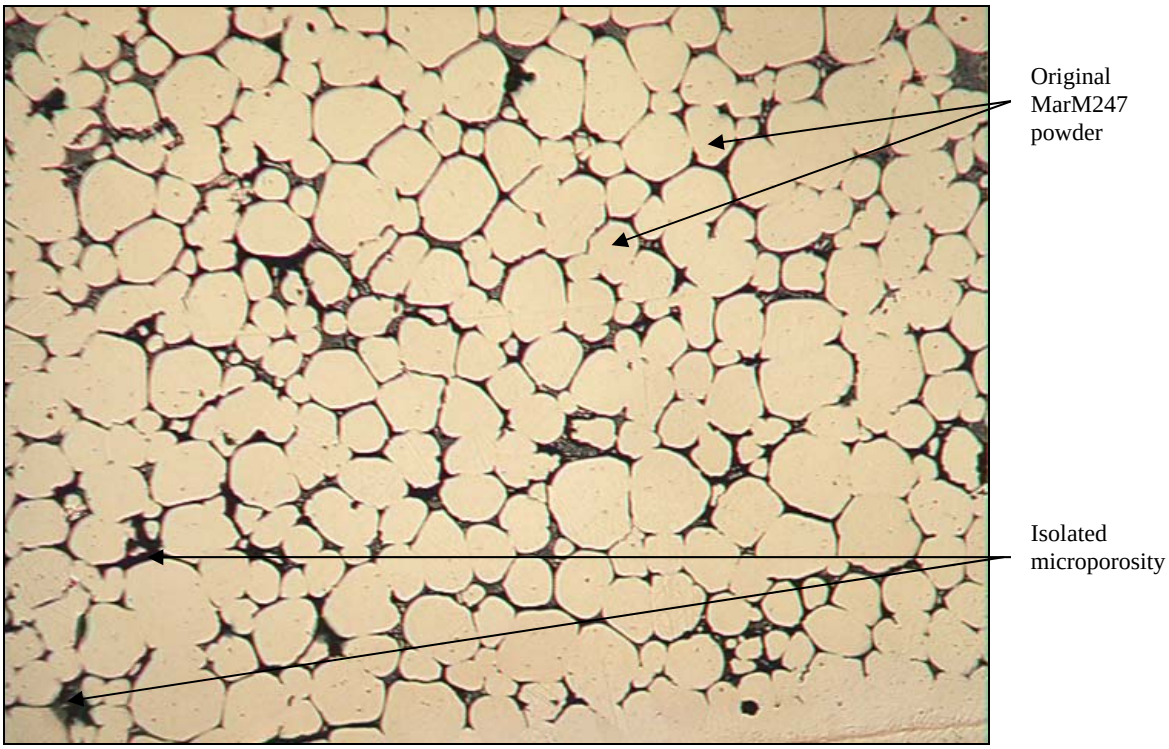

Figure 104 - Ni-Zr braze dispersed between MarM247 powder particles after brazing at 1230°C for 12 hours, followed by solution heat treatment at 1230°C for 4 hours and quenching. Magnification: 50X.

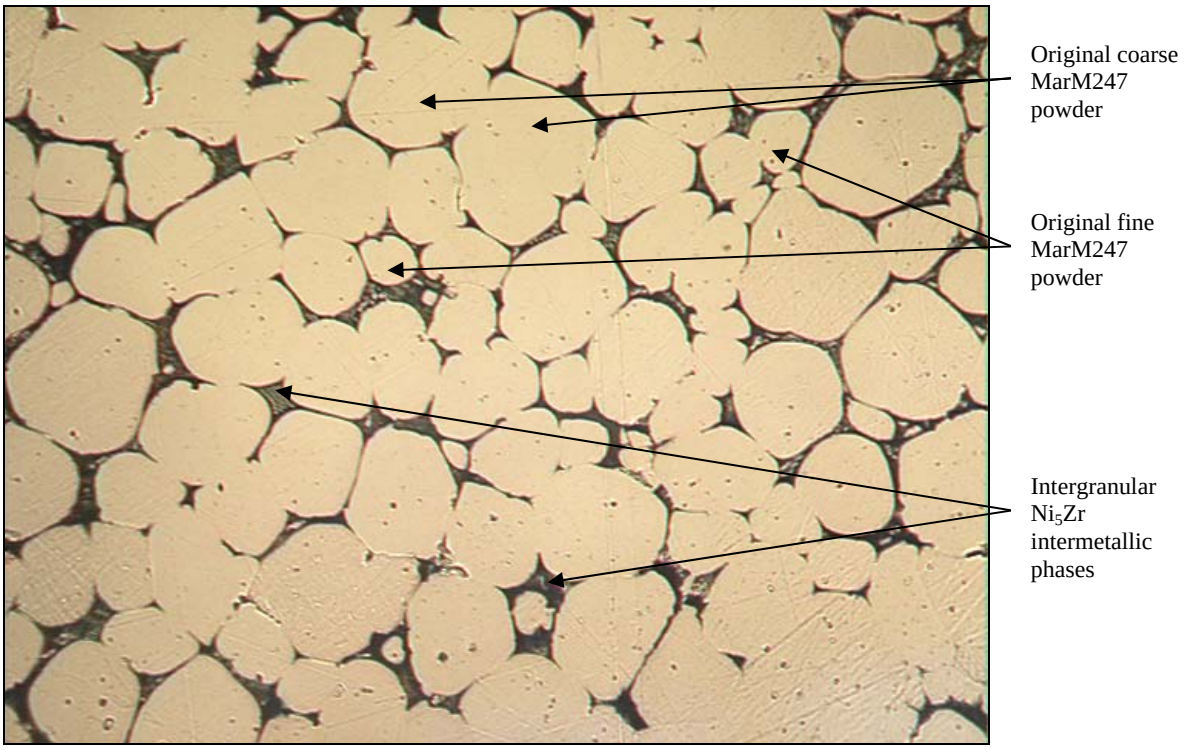

Figure 105 - Ni-Zr braze dispersed between MarM247 powder particles after brazing at 1230°C for 12 hours, followed by solution heat treatment at 1230°C for 4 hours and quenching. Magnification: 100X.

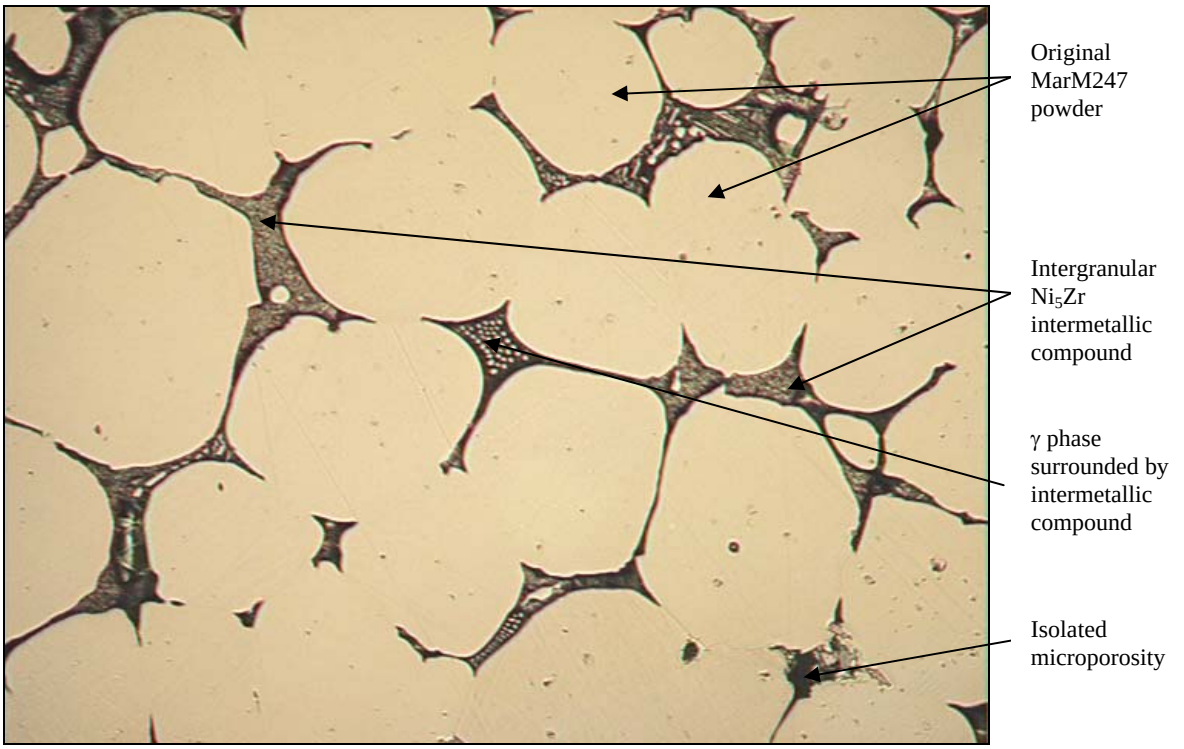

Figure 106 - Ni-Zr braze dispersed between MarM247 powder particles after brazing at 1230°C for 12 hours, followed by solution heat treatment at 1230°C for 4 hours and quenching. Magnification: 200X.

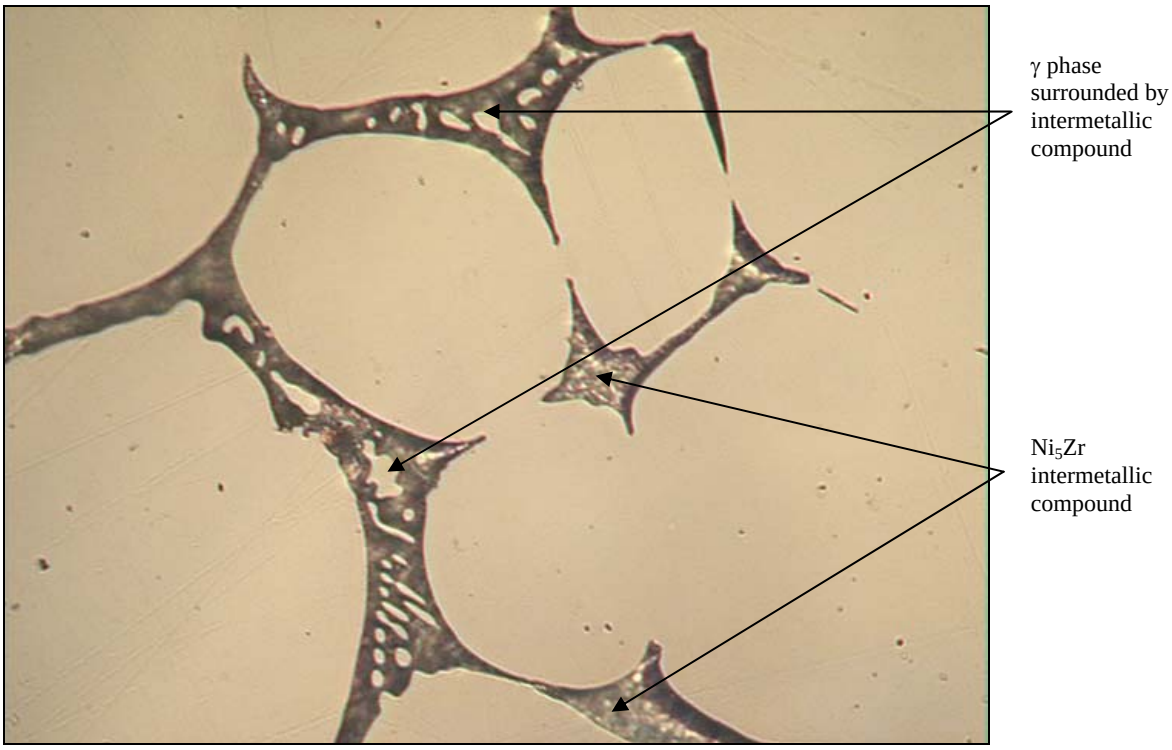

Figure 107 - Ni-Zr braze dispersed between MarM247 powder particles after brazing at 1230°C for 12 hours, followed by solution heat treatment at 1230°C for 4 hours and quenching. Magnification: 500X.

SEM micrographs of the Ni-Hf joint, processed at 1230°C for 12 hours, followed by solution heat treatment at 1230°C for 4 hours, are shown in **Figures 108 and 109**. Two phases within the original braze alloy were analyzed, indicated by the arrows in **Figure 108**. As indicated on the micrograph, one of these phases was identified as γ, consisting of 73.14Ni-6.33Co-7.37Cr-2.73Al-6.10W-1.49Mo-0.65Ti (wt.%). The phase surrounding the γ particles was identified as Ni_7Hf_2, with a composition of 52.96Ni-43.90Hf-2.18Co-0.46Cr-0.16Ti-0.34W (wt.%). The more angular intergranular phase, highlighted by the arrows in **Figure 109**, was shown to consist of 53.01Ni-43.09Hf-2.43Co-0.82Cr-0.20Ti-0.45W (wt.%), and was therefore also identified as Ni_7Hf_2.

Figures 110 and 111 display SEM micrographs of the Ni-Zr joint after processing at 1230°C for 12 hours, followed by solution annealing at 1230°C for 4 hours. Two of the intergranular phases in **Figure 110** were analyzed, as indicated by the arrows. One of these phases, consisting of 75.46Ni-5.27Co-5.23Cr-3.42Al-7.17W-1.16Fe-0.92Mo-0.70Ti-0.68Zr (wt%.), was identified as γ phase. The second phase had a composition of 73.63Ni-23.75Zr-2.09Co-0.53Al (wt.%), and was identified as Ni_5Zr. The intergranular phase highlighted by the arrows in **Figure 111** had a similar composition (70.78Ni-25.44Zr-2.27Co-0.81Cr-0.44Al-0.25W), and was therefore also identified as Ni_5Zr intermetallic compound.

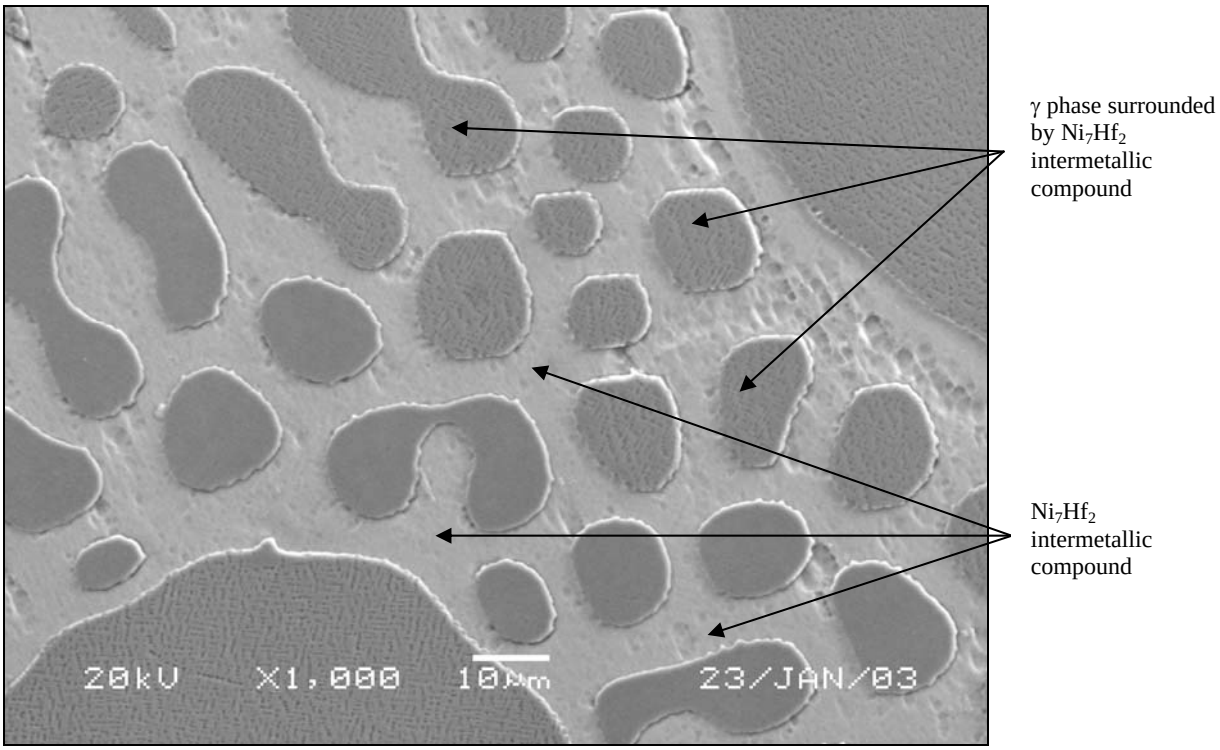

Figure 108 – SEM micrograph of the Ni-Hf braze, showing the phases identified as γ and Ni_7Hf_2.

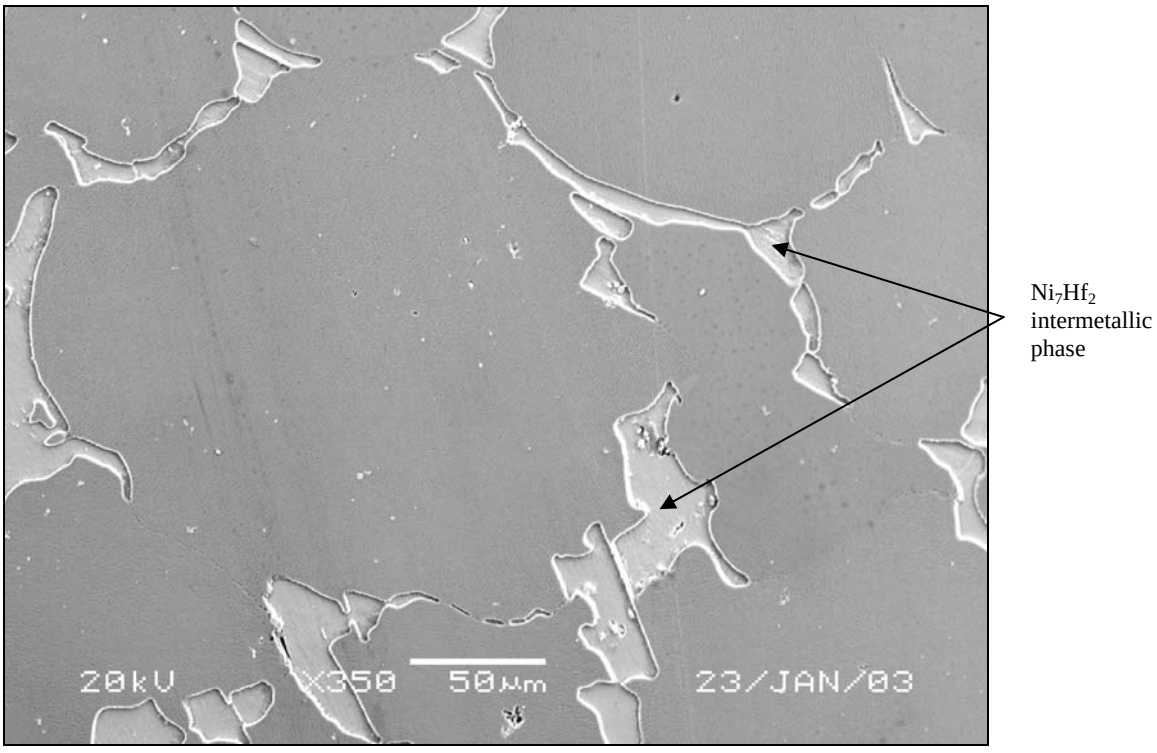

Figure 109 – SEM micrograph of the Ni-Hf braze, showing islands of intergranular Ni_7Hf_2 intermetallic compound.

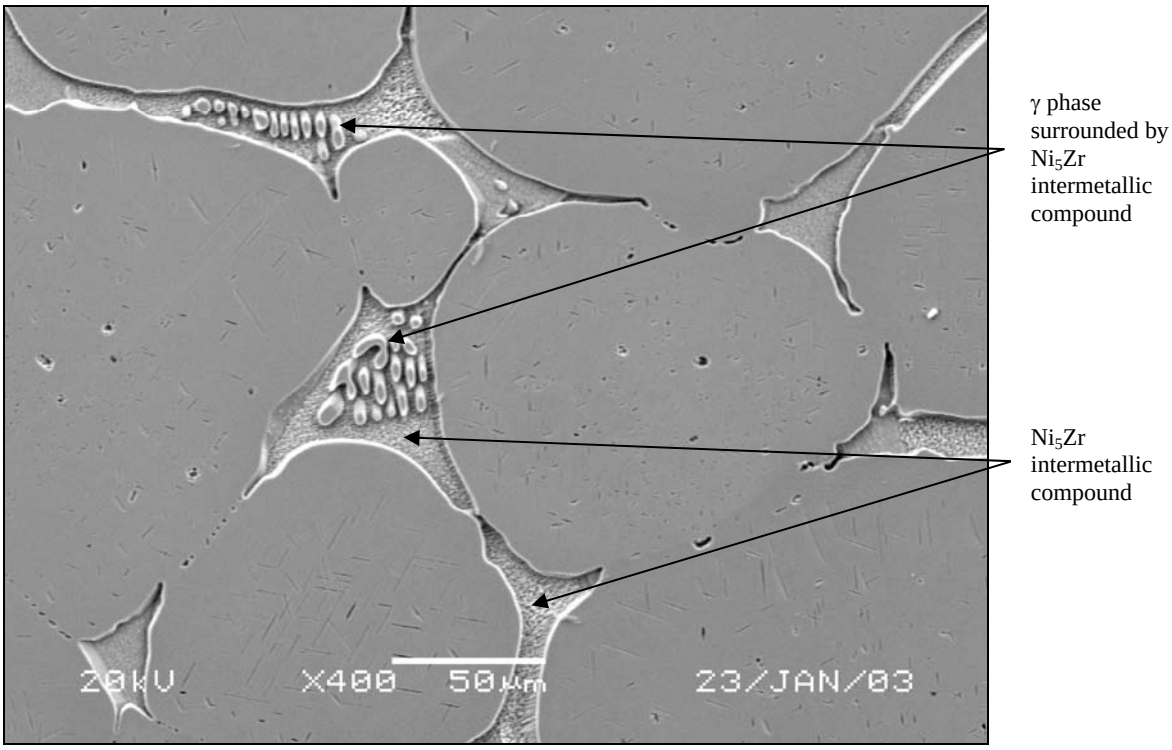

Figure 110 – SEM micrograph of the Ni-Zr braze, showing the phases identified as γ and Ni_5Zr.

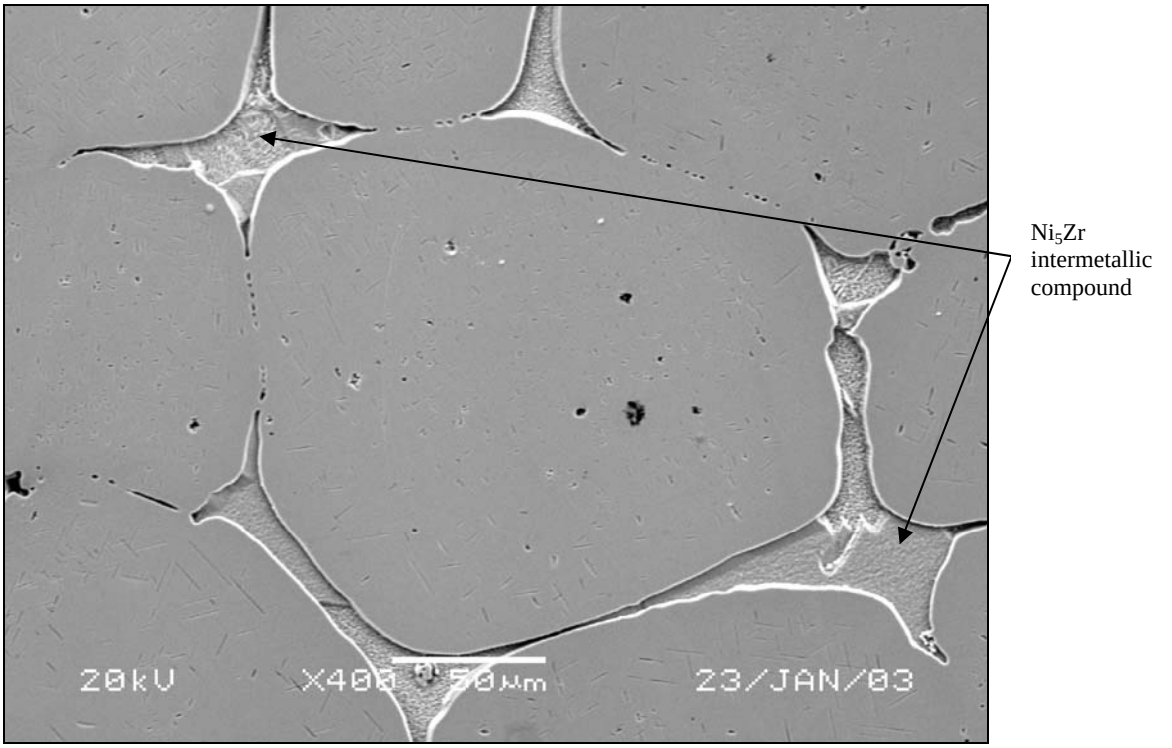

Figure 111 – SEM micrograph of the Ni-Zr braze, showing islands of intergranular Ni_5Zr intermetallic compound.

6.3.2 Creep rupture test results:

The results of creep rupture tests performed at three different stress levels at a temperature of 845°C are documented in **Table 24**, and displayed graphically in the form of a Larson-Miller plot in **Figure 112**. In **Table 24**, the creep rupture properties of the MarM247/Ni-Hf and MarM247/Ni-Zr joints are compared with those of the In738 base metal in the solution annealed condition.

Table 24 - Creep rupture properties at 845°C of the In738 base metal, and LPDB joints produced with MarM247 superalloy powder and Ni-Hf or Ni-Zr braze alloy. The test samples were produced with a joint gap of 1.5 mm to simulate a worst-case crack repair scenario.

Specimen identification	Failure location	Hours to failure	% Elongation	% Reduction in area
APPLIED STRESS 345 MPa (50 ksi)				
BM-1T (In738 as-cast base metal)	Base metal	30.0	5.0	7.0
BM-2T (In738 as-cast base metal)	Base metal	24.7	6.0	7.5
Average for the In738 as-cast base metal		**27.4**	**5.5**	**7.3**
738-1 (In738 brazed with MarM247/Ni-Zr)	Joint	20.5	3.6	4.6
738-2 (In738 brazed with MarM247/Ni-Zr)	Joint	21.8	3.0	4.0
738-3 (In738 brazed with MarM247/Ni-Zr)	Joint	20.9	3.7	4.7
Average for the MarM247/Ni-Zr joint		**21.1**	**3.4**	**4.4**
738-A (In738 brazed with MarM247/Ni-Hf)	Joint	20.6	3.7	5.8
738-B (In738 brazed with MarM247/Ni-Hf)	Joint	18.2	3.0	4.5
738-C (In738 brazed with MarM247/Ni-Hf)	Joint	17.0	4.5	6.5
Average for the MarM247/Ni-Hf joint		**18.6**	**3.7**	**5.6**
APPLIED STRESS 276 MPa (40 ksi)				
BM-3T (In738 as-cast base metal)	Base metal	100.0	6.2	8.7
BM-4T (In738 as-cast base metal)	Base metal	137.8	6.1	8.4
Average for the In738 as-cast base metal		**118.9**	**6.2**	**8.6**
738-4 (In738 brazed with MarM247/Ni-Zr)	Joint	75.2	5.7	8.6
738-5 (In738 brazed with MarM247/Ni-Zr)	Joint	78.8	3.9	7.9
738-6 (In738 brazed with MarM247/Ni-Zr)	Joint	70.1	4.9	7.2
Average for the MarM247/Ni-Zr joint		**74.7**	**4.8**	**7.9**
738-D (In738 brazed with MarM247/Ni-Hf)	Joint	73.2	4.9	7.6
738-E (In738 brazed with MarM247/Ni-Hf)	Joint	70.9	5.9	8.9
738-F (In738 brazed with MarM247/Ni-Hf)	Joint	68.9	5.2	8.4
Average for the MarM247/Ni-Hf joint		**71.0**	**5.3**	**8.3**
APPLIED STRESS 228 MPa (33 ksi)				
BM-5T (In738 as-cast base metal)	Base metal	200.0	6.6	8.8
BM-6T (In738 as-cast base metal)	Base metal	344.6	6.0	8.6
Average for the In738 as-cast base metal		**272.3**	**6.3**	**8.7**
738-7 (In738 brazed with MarM247/Ni-Zr)	Joint	253.6	4.2	6.0
738-8 (In738 brazed with MarM247/Ni-Zr)	Joint	240.0	4.4	6.3
738-9 (In738 brazed with MarM247/Ni-Zr)	Joint	232.2	4.9	6.7
Average for the MarM247/Ni-Zr joint		**241.9**	**4.5**	**6.3**
738-G (In738 brazed with MarM247/Ni-Hf)	Joint	209.8	5.3	7.5
738-H (In738 brazed with MarM247/Ni-Hf)	Joint	220.8	4.9	6.9
738-I (In738 brazed with MarM247/Ni-Hf)	Joint	214.3	5.2	7.0
Average for the MarM247/Ni-Hf joint		**215.0**	**5.1**	**7.1**

As shown in **Table 24**, the creep life to failure of the braze joints at 845°C was well below that of the In738 base metal at all three applied stress levels. At an applied stress level of 345 MPa, the MarM247/Ni-Zr and the MarM247/Ni-Hf braze joints achieved average creep lives to failure of approximately 77% and 68%, respectively, of that of the In738 base metal. At an applied stress level of 276 MPa, the creep life to failure of the joints was 63% and 60% of that of the base metal for the MarM247/Ni-Zr and MarM247/Ni-Hf joints, respectively. At 228 MPa, these values were 89% (Ni-Zr joints) and 79% (Ni-Hf joints) of the creep life determined for the In738 base metal. The Larson-Miller plot shown in **Figure 112** confirms that, compared to the MarM247/Ni-Hf joints, the MarM247/Ni-Zr braze joints displayed superior creep rupture properties at 845°C at all applied stress levels evaluated. In spite of the lower creep rupture properties of the MarM247/Ni-Hf braze joints, the ductility of these joints was marginally higher than that of the MarM247/Ni-Zr joints (as shown in **Table 24**).

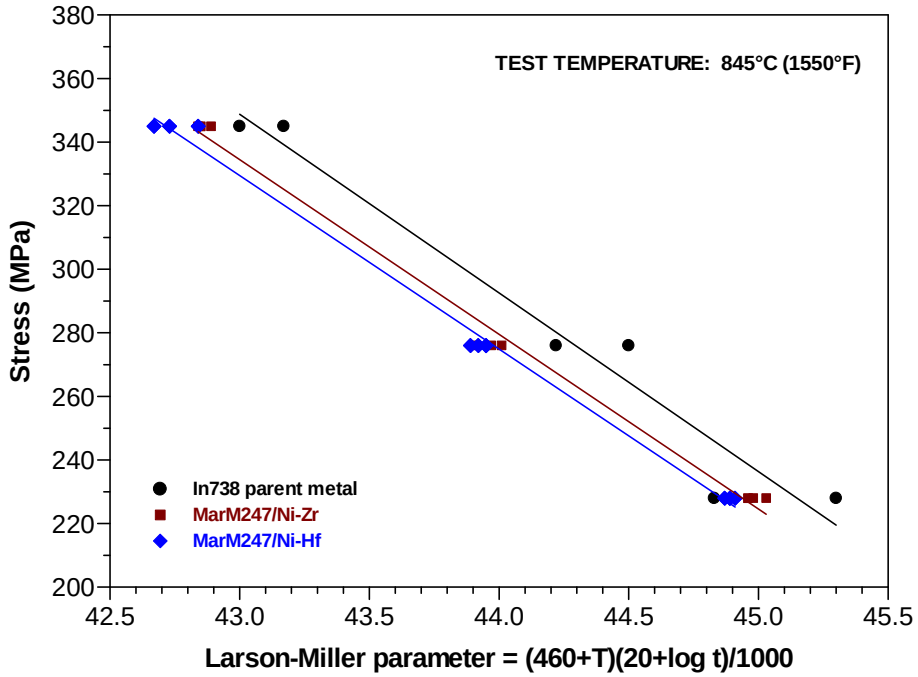

Figure 112 – Larson-Miller plot at 845°C for creep rupture tests performed at three applied stress levels: 345 MPa (50 ksi), 276 MPa (45 ksi) and 228 MPa (33 ksi) (where: *T* is temperature (°F) and *t* is time (hours)).

The creep rupture properties of the In738 base metal and the MarM247/Ni-Hf and MarM247/Ni-Zr joints at 900°C are shown in **Table 25**, and displayed graphically in the form of a Larson-Miller plot in **Figure 113**. The creep rupture lives of both braze joints were well below that of the parent metal at all three stress levels tested. At an applied stress of 242 MPa, the creep rupture life of the MarM247/Ni-Zr braze joint was 69% of that of the In738 base metal, whereas that of the MarM247/Ni-Hf braze joint was 64% of the base metal creep rupture life. At an applied stress of 186 MPa, the MarM247/Ni-Zr joint achieved 71%, and the MarM247/Ni-Hf joint 65%, of the creep rupture life of the In738 base metal. At 152 MPa, the creep rupture lives of the braze joints were 77% of the life of the base metal for the Ni-Zr braze, and 66% for the Ni-Hf braze. The Larson-Miller plot shown in **Figure 113** confirms that the MarM247/Ni-Zr braze joints outperformed the MarM247/Ni-Hf braze joints during creep rupture testing at 900°C. In spite of the lower creep rupture properties of the MarM247/Ni-Hf braze joints, the ductility of these joints was superior to that of the MarM247/Ni-Zr braze joints.

Table 25 - Creep rupture properties at 900°C of the In738 base metal, and LPDB joints produced with MarM247 superalloy powder and Ni-Hf or Ni-Zr braze alloy. The test samples were produced with a joint gap of 1.5 mm to simulate a worst-case crack repair scenario.

Specimen identification	Failure location	Hours to failure	% Elongation	% Reduction in area
APPLIED STRESS 242 MPa (35 ksi)				
BM-7T (In738 as-cast base metal)	Base metal	30.0	5.5	7.8
BM-8T (In738 as-cast base metal)	Base metal	29.5	5.9	7.9
Average for the In738 as-cast base metal		**29.8**	**5.7**	**7.9**
738-10 (In738 brazed with MarM247/Ni-Zr)	Joint	22.9	3.7	4.4
738-11 (In738 brazed with MarM247/Ni-Zr)	Joint	20.3	4.2	5.6
738-12 (In738 brazed with MarM247/Ni-Zr)	Joint	18.2	4.5	6.0
Average for the MarM247/Ni-Zr joint		**20.5**	**4.1**	**5.3**
738-J (In738 brazed with MarM247/Ni-Hf)	Joint	17.1	4.5	5.9
738-K (In738 brazed with MarM247/Ni-Hf)	Joint	19.4	4.6	6.1
738-L (In738 brazed with MarM247/Ni-Hf)	Joint	20.5	4.7	6.2
Average for the MarM247/Ni-Hf joint		**19.0**	**4.6**	**6.1**
APPLIED STRESS 186 MPa (27 ksi)				
BM-9T (In738 as-cast base metal)	Base metal	100.0	7.0	10.0
BM-10T (In738 as-cast base metal)	Base metal	109.1	6.9	9.9
Average for the In738 as-cast base metal		**104.6**	**7.0**	**9.9**
738-13 (In738 brazed with MarM247/Ni-Zr)	Joint	75.5	4.2	7.3
738-14 (In738 brazed with MarM247/Ni-Zr)	Joint	72.0	4.0	6.8
738-15 (In738 brazed with MarM247/Ni-Zr)	Joint	76.2	4.6	7.7
Average for the MarM247/Ni-Zr joint		**74.6**	**4.3**	**7.3**
738-M (In738 brazed with MarM247/Ni-Hf)	Joint	70.3	5.0	6.8
738-N (In738 brazed with MarM247/Ni-Hf)	Joint	69.2	5.6	8.0
738-O (In738 brazed with MarM247/Ni-Hf)	Joint	64.2	5.8	8.2
Average for the MarM247/Ni-Hf joint		**67.9**	**5.5**	**7.7**
APPLIED STRESS 152 MPa (22 ksi)				
BM-11T (In738 as-cast base metal)	Base metal	200.0	8.5	10.8
BM-12T (In738 as-cast base metal)	Base metal	404.2	8.0	10.0
Average for the In738 as-cast base metal		**302.1**	**8.3**	**10.4**
738-16 (In738 brazed with MarM247/Ni-Zr)	Joint	242.2	4.8	7.6
738-17 (In738 brazed with MarM247/Ni-Zr)	Joint	238.6	4.4	6.4
738-18 (In738 brazed with MarM247/Ni-Zr)	Joint	217.4	4.0	6.1
Average for the MarM247/Ni-Zr joint		**232.7**	**4.6**	**6.7**
738-G (In738 brazed with MarM247/Ni-Hf)	Joint	205.9	5.0	7.7
738-H (In738 brazed with MarM247/Ni-Hf)	Joint	198.4	5.5	7.8
738-I (In738 brazed with MarM247/Ni-Hf)	Joint	192.8	5.7	8.0
Average for the MarM247/Ni-Hf joint		**199.0**	**5.4**	**7.8**

The creep rupture properties of the In738 base metal, and the MarM247/Ni-Zr and MarM247/Ni-Hf joints measured at 980°C are displayed in **Table 26**, and shown graphically in the form of a Larson-Miller plot in **Figure 114**. At an applied stress level of 138 MPa, the creep rupture life of the MarM247/Ni-Zr joint was 79% of the creep rupture life of the base metal, and that of the MarM247/Ni-Hf joint 64%. These values decreased to 70% and 61% of the creep rupture life of the base metal, respectively, for the MarM247/Ni-Zr and

MarM247/Ni-Hf joints at an applied stress level of 104 MPa. The creep rupture life of the Ni-Zr joint at an applied stress of 76 MPa was 81% of that of the In738 base metal, whereas that of the Ni-Hf braze joint achieved 78% of creep rupture life of the base metal. The Larson-Miller plot shown in **Figure 114** indicates that the creep rupture properties of the MarM247/Ni-Zr braze joints were superior to those of MarM247/Ni-Hf brazed joints. The MarM247/Ni-Hf joints, however, displayed superior ductility at all stress levels. The average percentage elongation and percentage reduction in area of the MarM247/Ni-Hf brazed joints were 73% and 70% of those of the base metal, respectively, whereas the MarM247/Ni-Zr brazed joints displayed approximately 60% of the ductility of the base metal.

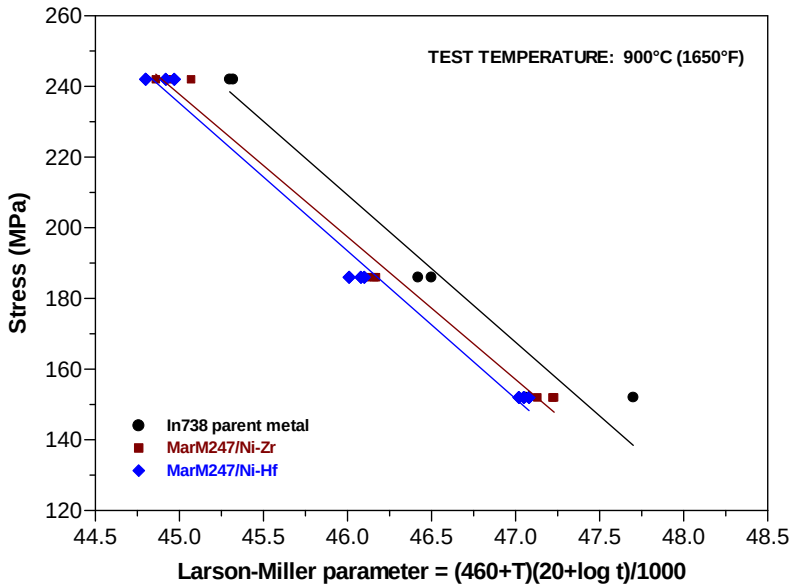

Figure 113 –Larson-Miller plot at 900°C for creep rupture tests performed at three applied stress levels: 242 MPa (35 ksi), 186 MPa (27 ksi) and 152 MPa (22 ksi) (where: *T* is temperature (°F) and *t* is time (hours)).

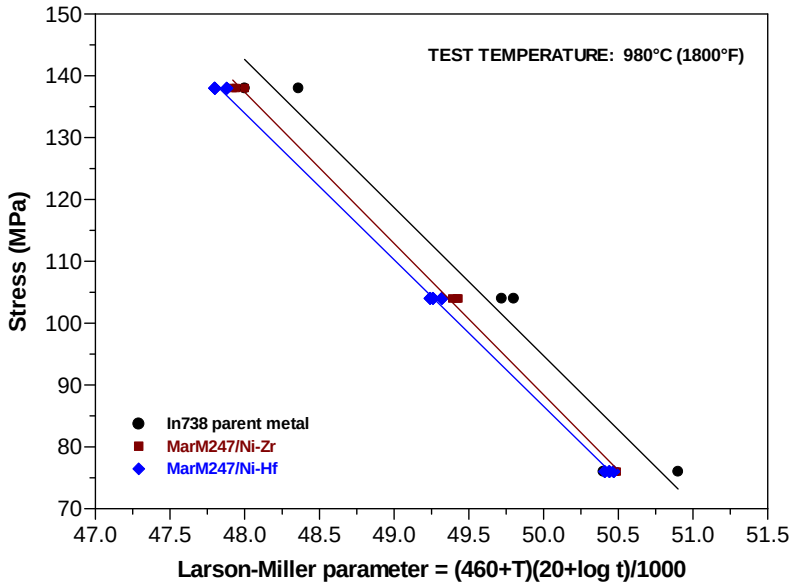

Figure 114 –Larson-Miller plot at 980°C for creep rupture tests performed at three applied stress levels: 138 MPa (20 ksi), 104 MPa (15 ksi) and 76 MPa (11 ksi) (where: *T* is temperature (°F) and *t* is time (hours)).

Table 26 - Creep rupture properties at 980°C of the In738 base metal, and LPDB joints produced with MarM247 superalloy powder and Ni-Hf or Ni-Zr braze alloy. The test samples were produced with a joint gap of 1.5 mm to simulate a worst-case crack repair scenario.

Specimen identification	Failure location	Hours to failure	% Elongation	% Reduction in area
APPLIED STRESS 138 MPa (20 ksi)				
BM-13T (In738 as-cast base metal)	Base metal	25.0	8.0	11.6
BM-14T (In738 as-cast base metal)	Base metal	17.3	8.2	11.9
Average for the In738 as-cast base metal		**21.2**	**8.1**	**11.8**
738-19 (In738 brazed with MarM247/Ni-Zr)	Joint	15.9	5.6	7.5
738-20 (In738 brazed with MarM247/Ni-Zr)	Joint	16.3	5.2	7.0
738-21 (In738 brazed with MarM247/Ni-Zr)	Joint	17.3	4.5	6.9
Average for the MarM247/Ni-Zr joint		**16.5**	**5.1**	**7.1**
738-S (In738 brazed with MarM247/Ni-Hf)	Joint	15.3	6.1	8.8
738-T (In738 brazed with MarM247/Ni-Hf)	Joint	14.1	6.7	9.3
738-U (In738 brazed with MarM247/Ni-Hf)	Joint	11.3	6.9	9.9
Average for the MarM247/Ni-Hf joint		**13.6**	**6.6**	**9.3**
APPLIED STRESS 104 MPa (15 ksi)				
BM-15T (In738 as-cast base metal)	Base metal	100.0	8.1	11.9
BM-16T (In738 as-cast base metal)	Base metal	108.5	8.2	12.1
Average for the In738 as-cast base metal		**104.3**	**8.2**	**12.0**
738-22 (In738 brazed with MarM247/Ni-Zr)	Joint	73.3	4.3	7.0
738-23 (In738 brazed with MarM247/Ni-Zr)	Joint	74.2	4.0	6.8
738-24 (In738 brazed with MarM247/Ni-Zr)	Joint	71.4	4.9	7.4
Average for the MarM247/Ni-Zr joint		**73.0**	**4.4**	**7.1**
738-V (In738 brazed with MarM247/Ni-Hf)	Joint	61.5	5.7	7.6
738-W (In738 brazed with MarM247/Ni-Hf)	Joint	66.6	5.1	7.0
738-X (In738 brazed with MarM247/Ni-Hf)	Joint	62.5	5.6	7.4
Average for the MarM247/Ni-Hf joint		**63.5**	**5.5**	**7.3**
APPLIED STRESS 76 MPa (11 ksi)				
BM-17T (In738 as-cast base metal)	Base metal	200.0	8.8	12.9
BM-18T (In738 as-cast base metal)	Base metal	332.8	8.6	12.4
Average for the In738 as-cast base metal		**266.4**	**8.7**	**12.7**
738-25 (In738 brazed with MarM247/Ni-Zr)	Joint	214.7	5.9	8.2
738-26 (In738 brazed with MarM247/Ni-Zr)	Joint	218.8	5.0	7.0
738-27 (In738 brazed with MarM247/Ni-Zr)	Joint	216.1	5.4	7.3
Average for the MarM247/Ni-Zr joint		**216.5**	**5.4**	**7.5**
738-Y (In738 brazed with MarM247/Ni-Hf)	Joint	202.6	6.2	8.9
738-Z (In738 brazed with MarM247/Ni-Hf)	Joint	214.8	6.0	8.6
738-ZZ (In738 brazed with MarM247/Ni-Hf)	Joint	208.0	6.1	8.7
Average for the MarM247/Ni-Hf joint		**208.5**	**6.1**	**8.7**

The Larson-Miller plots shown in **Figures 112 to 114** were constructed individually for each of the three test temperatures. In order to compare the creep rupture test data at all three test temperatures, the data shown in **Tables 24 to 26** were combined into a single Larson-Miller plot, shown in **Figure 115**. Based on this figure, the three materials were ranked in descending order of creep rupture properties: In738 base metal, the MarM247/Ni-Zr braze joint, and the MarM247/Ni-Hf joint. It must be emphasized, however, that linear regression

methods revealed no statistically relevant differences between the Larson-Miller plots of the MarM247/Ni-Zr and MarM247/Ni-Hf braze joints.

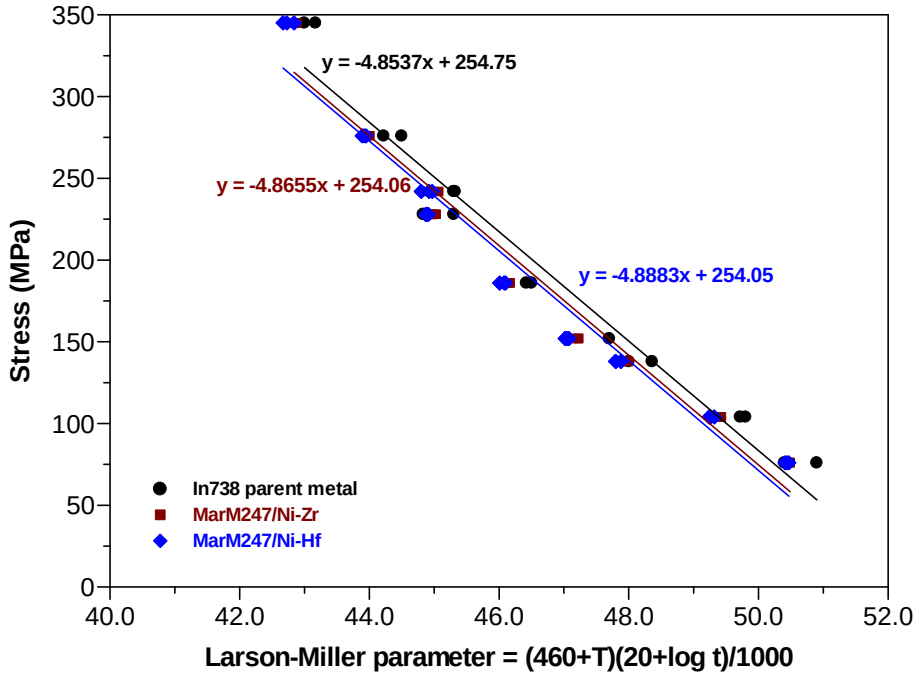

Figure 115 – Larson-Miller plot for the In738 base metal, the MarM247/Ni-Zr joint and the MarM247/Ni-Hf braze joints in the solution annealed condition.

6.4) Conclusions

- A relatively dense, low porosity LPDB joint, with a microstructure consisting of MarM247 powder particles surrounded by Ni-Hf or Ni-Zr braze alloy, formed during processing at 1230°C for 12 hours, followed by solution heat treatment at 1230°C for 4 hours. The braze microstructure consisted of γ dendrites, surrounded by Ni_5Zr or Ni_7Hf_2 intermetallic compound, interspersed with more continuous regions of Ni_5Zr or Ni_7Hf_2 intermetallic compound.

- The extended brazing cycle further reduced the amount of γ and Ni_5Zr/Ni_7Hf_2 intermetallic compound, and decreased the thickness of the layers of braze alloy surrounding the MarM247 powder particles.

- Creep rupture tests performed at 845°C, 900°C and 980°C at various stress levels revealed that the MarM247/Ni-Zr brazed joints have superior creep rupture properties compared with the MarM247/Ni-Hf joints. A combined Larson Miller plot, however, showed little statistically relevant difference between the creep rupture properties of the two braze filler metals in the solution annealed condition.

- The creep rupture properties described in this chapter were measured in the solution annealed condition and should improve following a suitable aging heat treatment. In the solution heat treated condition, the creep rupture properties of the Ni-Hf and Ni-Zr joints achieved between 65% and 75% of the creep rupture properties of the In738 base metal. Based on past experience with brazed joints using a Ni-B braze alloy, the aging treatment is expected to improve the creep rupture properties by between 15% and 20%.

- The ductility of the Ni-Hf braze joints was higher than that of the Ni-Zr joints. The joint ductility is expected to decrease marginally following aging heat treatment.

- The results presented in this chapter were obtained after processing times of 12 hours, followed by solution heat treatment for an additional 4 hours. Promising joint microstructures and creep rupture properties were obtained, but isolated microporosity was observed in the Ni-Zr and Ni-Hf joints. In order to improve the joint quality, Hot Isostatic Pressing (HIP'ing) was used in an attempt to close the micropores that form during the braze cycle. Chapter 7 describes the influence of such a HIP cycle on the microstructure and amount of microporosity in MarM247/Ni-Hf and MarM247/Ni-Zr joints after brazing for 12 hours at 1230°C, followed by a solution annealing treatment.